J|A|C|S
ARTICLES
Published on Web 11/14/2007

Isostable DNA

Carolin Ahlborn, Karsten Siegmund, and Clemens Richert*

Contribution from the Institut für Organische Chemie, Universität Karlsruhe (TH), Karlsruhe, Germany

Received June 22, 2007; E-mail: cr@rrg.uka.de

Abstract: The high fidelity detection of multiple DNA sequences in multiplex assays calls for duplexes whose stability is independent of sequence (isostable DNA), forming under universally stringent conditions. Nature did not evolve DNA to form isostable duplexes. Here we report how probe strands can be modified so that an all-A/T target strand is bound with the same or slightly higher affinity than the corresponding all-G/C strand with the same sequence of purines and pyrimidines. We refer to these probes that feature covalently attached ligands as "decorated nucleic acids". Caps, intercalators, and locks were used to stabilize A/T duplexes, and *N*4-ethylcytosine residues were employed to tune down the stability of G/C duplexes without significantly affecting base pairing selectivity. Near-isostability was demonstrated in solution and on microarrays of high and low density. Further, it is shown that hybridization results involving decorated probes on microarrays can be predicted on the basis of thermodynamic data for duplex formation in solution. Predictable formation of isostable DNA not only benefits microarrays for gene expression analysis and genotyping, but may also improve the sequence-specificity of other applications that rely on the massively parallel formation of Watson−Crick duplexes.

Introduction

Nature evolved DNA that features two types of base pairs. Guanine and cytosine form strong base pairs with three hydrogen bonds and stabilizing secondary electrostatic interactions.[1] Adenine and thymine form weak base pairs with two hydrogen bonds and no favorable secondary interactions. The binding constant is approximately 3 orders of magnitude larger for G:C base pairs than for A:U base pairs.[2] The differences in base-pair stability serve important roles in cells. For example, A/T-rich sequence motifs ("TATA boxes") are found at the start locus of genes, where strands have to be separated.[3] Other A/T-rich elements are sites for preferred recombination in plants.[4] Sequences that are rich in G and C are found in regions of the genome critical for regulating gene expression,[5] where stable duplexes are advantageous. Other motifs with high G/C content are inverted repeats[6] and GC islands.[7] Patterns of AA/TT dinucleotides and GC dinucleotides induce a curvature in DNA that favors nucleosome formation.[8] Finally, some bacteria and archea adjust duplex stability according to the temperature of their environment[9] by tuning the G/C content of their genome. This would be impossible, if their genetic material was made up of base pairs with equal stability.

While beneficial for its natural roles, the dependence of duplex stability on G/C content can be problematic for biomedical applications of DNA. Such applications include use as hybridization probe, primer, sequencing probe,[10] antisense[11] or antigene agent,[12] and as component for nanotechnology and material sciences.[13−15] For many uses of DNA, sequence selectivity is critical. Perhaps most demanding is the massively parallel detection of target strands on DNA microarrays. On current high-density microarrays, $>10^5$ different duplexes have to form simultaneously.[16] The growth in total spot number and density on microarrays continues unabated, and more demanding applications are being tackled with microarrays,[17,18] including SNP genotyping,[19−21] which requires discrimination between target strands differing in a single nucleotide.

(1) Pranata, J.; Wierschke, S. G.; Jorgensen, W. L. *J. Am. Chem. Soc.* **1991**, *113*, 2810−2819.
(2) Kyogoku, Y.; Lord, R. C.; Rich, A. *Biochim. Biophys. Acta* **1969**, *179*, 10−17.
(3) Voet, D.; Voet, J. G. *Biochemistry*, 2nd ed.; J. Wiley & Sons, New York, 1995.
(4) Müller, A. E.; Kamisugi, Y.; Grüneberg, R.; Niedenhof, I.; Hörold, R. J.; Meyer, P. *J. Mol. Biol.* **1999**, *291*, 29−46.
(5) Hapgood, J. P.; Riedemann, J.; Scherer, S. D. *Cell Biol. Intern.* **2001**, *25*, 17−31.
(6) Ruskin, B.; Fink, G. R. *Genetics* **1993**, *133*, 43−56.
(7) Welm, A. L.; Mackey, S. L.; Timchemko, L. T.; Darlington, G. J.; Timchenko, N. A. *J. Biol. Chem.* **2000**, *275*, 27406−27413.
(8) Istvan, A.; Marvich, T. N.; Tomsho, L. P.; Qi, J.; Zanton, S. J.; Schuster, S. C.; Pugh, B. F. *Nature* **2007**, *446*, 572−576.
(9) Nelson, K. E.; Paulsen, I. T.; Heidelberg, J. F.; Fraser, C. M. *Nat. Biotechnol.* **2000**, *18*, 1049−1054.
(10) Shendure, J.; Porreca, G. J.; Reppas, N. B.; Lin, X.; McCutheon, J. P.; Rosenbaum, A. M.; Wang, M. D.; Zhang, K.; Mitra, R. D.; Church, G. M. *Science* **2005**, *309*, 1728−1732.
(11) Uhlmann, E.; Peyman, A. *Chem. Rev.* **1990**, *90*, 543−584.
(12) Praseuth, D.; Guieysse, A. L.; Hélène, C. *Biochim. Biophys. Acta* **1999**, *1489*, 181−206.
(13) Park, S. H.; Yin, P.; Liu, Y.; Reif, J. H.; LaBean, T. H.; Yan, H. *Nano Lett.* **2005**, *5*, 729−733.
(14) Rothemund, P. W. K. *Nature* **2006**, *440*, 297−302.
(15) Feldkamp, U.; Niemeyer, C. M. *Angew. Chem., Int. Ed.* **2006**, *45*, 1856−1876.
(16) Pennisi, E. *Science* **2003**, *302*, 211.
(17) Waldman, M. *Nature* **2006**, *444*, 256.
(18) Schumacher, A.; Kapranov, P.; Kaminsky, Z.; Flanagan, J.; Assadzadeh, A.; Yau, P.; Virtanen, C.; Winegarden, N.; Cheng, J.; Gingeras, T.; Petronis, A. *Nucleic Acids Res.* **2006**, *34*, 528−542.

10.1021/ja074209p CCC: $37.00

Even as "enabling technique", DNA microarray assays suffer from challenges, such as reproducibility and calibration,[22−25] as highlighted in comparative studies.[26−28] Perhaps the most important challenge is low fidelity caused by cross-hybridization, i.e., binding of target strands to probes that are not fully complementary.[29] This phenomenon causes false positive signals and/or exaggerated signals at spots with related sequences.[30] Cross-hybridization also draws target strands away from the spot with the fully complementary probes, lowering signal intensity at this spot. Minimizing false positive results by using more stringent hybridization and washing conditions necessarily increases the likelihood of false negative results for duplexes of low stability. The different stability of A:T and G:C base pairs is thus the molecular basis of a key factor that limits the fidelity of massively parallel detection.

To counter the effect of base pairing strength, probe design for microarrays usually includes the selection of sequences with an appropriate G/C content, using computer algorithms,[31] but this narrows the accessible sequence space, particularly for members of gene families formed through gene duplication. In a confined sequence space, cross-hybridization becomes more likely. On some commercial microarrays, control sequences differing by a single nucleotide are employed, but using the signal they produce for background subtraction is known to be problematic.[32] Single mismatches cause different drops in free energy of binding, depending on sequence context and position in a duplex.[33,34] That the physical limits of selective molecular recognition are readily reached can be demonstrated in simulations. The spread of melting points between probe/target duplexes can be >20 °C for a commercial DNA microarray,[35] corroborating concerns that melting points will necessarily differ over a wide range in mixtures with sequences of varying G/C-content.[36]

The extent to which detection of target strands can be affected by base composition may be demonstrated for a specific sequence of purines and pyrimidines, such as 5′-TAATTTT-TAATAAT-3′ and 5′-CGGCCCCCGGCGGC-3′, whose duplexes melt more than 40 °C apart from each other (vide infra). This difference in melting points is much greater than the ≤20 °C drop in melting point caused by a single mismatch. This is true even when the mismatch is at the center of the sequence. No temperature exists at which both sequences bind their targets single base selectively, and at an intermediate temperature neither the all-G/C sequence nor the all-A/T sequence shows single-base specific binding (Figure 1a).

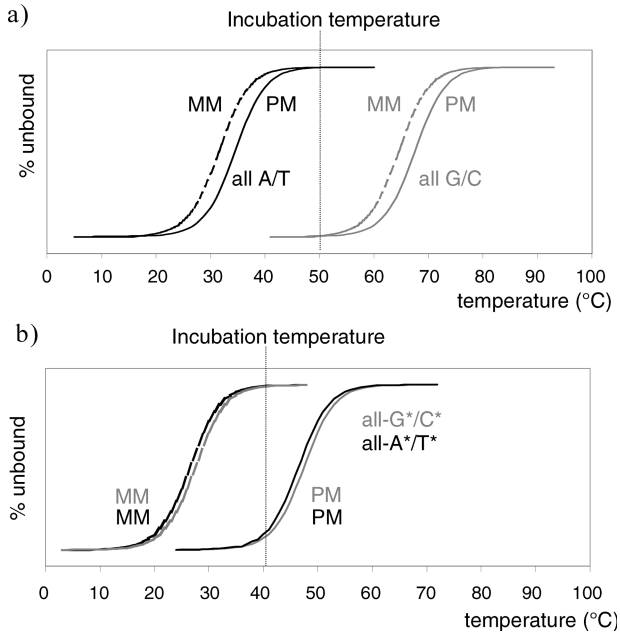

Figure 1. Cartoons of binding curves for probes containing a high G/C content or a high A/T content on (a) a conventional and (b) a chemically optimized DNA microarray. Curves for perfectly matched duplexes (PM, solid lines) and those with a single mismatch (MM, broken lines) are shown. An intermediate hybridization temperature in panel a leads to a false negative result for the A/T-rich sequence and to a lack of base pairing fidelity for the G/C-rich sequence. For panel b, with modified residues (A*, C*, G*, and T*) PM targets of any sequence are bound with similar affinity, and any mismatched base in a target leads to a drop in affinity.

Given the limitations of natural DNA, it is desirable to adjust duplex stability by chemically modifying probes, rather than confining oneself in the available sequence space. Oligonucleotides that give duplex stabilities independent of sequence (isostable DNA) can be expected to be superior hybridization probes in multiplexing experiments. With binding curves of the kind shown in Figure 1b, at an optimized temperature, all perfectly matched targets will be bound, but mismatched targets will remain essentially unbound for all spots of a microarray. The "ideal chip" scenario also requires accurate prediction of binding curves, so that conditions that ensure maximum fidelity can be chosen without iteration.[37]

Despite numerous biological studies involving DNA microarrays,[38] much of the chemical research on microarrays has focused on the linkers to the surface and protecting groups for photolithographic syntheses.[39,40] Few reports on chemically adjusting the target affinity of DNA probes to isostability can be found in the literature.[41,42] To the best of our knowledge, truly isostable DNA has not yet been demonstrated, nor has

(19) Kennedy, G. C.; et al. *Nat. Biotechnol.* **2003**, *21*, 1233−1237.
(20) Matsuzaki, H.; et al. *Genome Res.* **2004**, *14*, 414−425.
(21) Gresham, D.; Ruderfer, D. M; Pratt, S. C.; Schacherer, J.; Dunham, M. J.; Botstein, D.; Kruglyak, L. *Science* **2006**, *311*, 1932−1936.
(22) Lee, M. L. T.; Kuo, F. C.; Whitmore, G. A.; Sklar, J. *Proc. Natl. Acad. Sci. U.S.A.* **2000**, *97*, 9834−9839.
(23) Jenssen, T. K.; Langaas, M.; Kuo, W. P.; Sørensen, B. S.; Myklebost, O.; Hovig, E. *Nucleic Acids Res.* **2002**, *30*, 3235−3244.
(24) Kothapalli, R.; Yoder, S. J.; Mane, S.; Loughran, Jr., T. P. *BMC Bioinformatics* **2002**, *3*, 22.
(25) Draghici, S.; Khatri, P.; Eklund, A. C.; Szallasi, Z. *Trends Genet.* **2006**, *22*, 101−109.
(26) Iacobuzio-Donahue, C. A.; Ashafq, R.; Maitra, A.; Adsay, N. V.; Sheng-Ong, G. L.; Berg, K.; Hollingsworth, M. A.; Cameron, J. L.; Yeo, C. J.; Kern, S. E.; Goggins, M.; Hurban, R. H. *Cancer Res.* **2003**, *63*, 8614−8622.
(27) Tan, P. K.; Downey, T. J.; Spitznagel, E. L.; Xu, P.; Fu, D.; Dimitrov, D. S.; Lempicki, R. A.; Raaka, B. M.; Cam, M. C. *Nucleic Acids Res.* **2003**, *31*, 5676−5684.
(28) Cao, W.; et al. *BMC Genomics* **2004**, *5*, 26.
(29) Marshall, E. *Science* **2004**, *306*, 630−631.
(30) Plutowski, U.; Richert, C. *Angew. Chem., Int. Ed.* **2005**, *44*, 621−625.
(31) Li, X. Y.; He, Z. L.; Zhou, J. Z. *Nucleic Acids Res.* **2005**, *33*, 6114−6123 and references therein.
(32) Irizarry, R. A.; Bolstad, B. M.; Collin, F.; Cope, L. M.; Hobbs, B.; Speed, T. P. *Nucleic Acids Res.* **2003**, *31*, e15.
(33) Hong, B. J.; Sunkara, V.; Park, J. W. *Nucleic Acids Res.* **2005**, *33*, e106.
(34) Zhang, L.; Wu, C.; Carta, R.; Zhao, H. *Nucleic Acids Res.* **2007**, *35*, e18.
(35) Siegmund, K.; Ahlborn, C.; Richert, C., submitted for publication. The program ChipCheckII can be accessed at http://chipcheck.chemie.uni-karlsruhe.de/ and can be made available for download upon request.
(36) Southern, E.; Mir, K.; Shchepinov, M. *Nat. Genet.* **1999**, *21*, 5−9.
(37) Urakawa, H.; El Fantroussi, S.; Smidt, H.; Smoot, J. C.; Tribou, E. H.; Kelly, J. J.; Noble, P. A.;. Stahl D. A. *Appl. Environ. Microbiol.* **2003**, *69*, 2848−2856.
(38) Dalma-Weiszhausz, D. D.; Warrington, J.; Tanimoto, E. Y.; Miyada, G. *Methods Enzym.* **2006**, *410*, 3−28, and references therein.
(39) Niemeyer, C. M.; Blohm, D. *Angew. Chem., Int. Ed.* **1999**, *38*, 2865−2869.
(40) Pirrung, M. C. *Angew. Chem., Int. Ed.* **2002**, *41*, 1277−1289.

such DNA been employed on microarrays. Here we show how duplex stability can be adjusted such that an all-A/T tetradecamer sequence is bound with the same or slightly higher affinity than its all-G/C counterpart, leading to signals of similar intensity on DNA microarrays.

Results

In the first phase of our study, we focused on enhancing the stability of T:A base pairs. Several approaches for stabilizing A:T and T:A base pairs are known from the literature. An additional hydrogen bond can be introduced in these base pairs by employing a diaminopurine derivative as replacement for adenine, as demonstrated by Seela and co-workers.[43] A similar effect is difficult to realize for thymidine, as adenines in the target strands do not offer a third hydrogen-bonding functionality on their Watson−Crick base-pairing face. Backbone-modified oligonucleotides are known to increase duplex stability, including peptide nucleic acids (PNA),[44,45] but these are difficult to combine freely with unmodified DNA. Locked nucleic acids (LNA)[46] do not have this disadvantage[47] and have been recommended for gene expression profiling applications.[48] Other DNA backbone modifications can give duplexes with increased thermal stability, but are less readily incorporated during conventional synthesis cycles and are not readily available commercially. These include *N*3′-*P*5′-phosphoramidates,[49] guanidinium nucleic acids (DNG),[50] and 1′,5′-anhydrohexitol nucleic acids.[51] For RNA as target strand, data on backbone-modified oligonucleotide derivatives that form duplexes of increased stability are available, mostly from studies on antisense inhibition of gene expression,[11,52,53,54] but it is not clear how easily they can be applied to microarrays.

We selected DNA derivatives that retain the entire framework of natural DNA and are solely stabilizing through additional interactions mediated by substituents (rather than replacements of the DNA backbone or nucleobases) to avoid the high propensity of non-ionic analogues to form alternative structures.[55,56] We term such ligand-enforced oligonucleotides "decorated nucleic acids." They have the advantage of being fully compatible with automated DNA synthesis, a feature deemed critical for application in industrial microarray fabrication. This ensures that substituents may be strategically placed anywhere in a probe sequence via established methods possibly including photolithographic syntheses.[57,39] The decorated DNA can be expected to engage in more extensive interactions with the target structure than unmodified DNA, interrogating its structure (and thus its sequence) more thoroughly.

Target strands without modifications (other than fluorophore labeling at the terminus) were to be employed in our study to ensure that DNA from biological sources or amplified via inexpensive PCR with unmodified dNTPs may be detected. To generate A/T-rich duplexes with sufficiently high thermal stability, we combined duplex-stabilizing modifications in the interior with "molecular caps"[58] at either terminus of the hybridization probes. Caps are non-nucleosidic substituents that increase duplex stability and base-pairing fidelity at the termini by bridging canonical terminal base pairs much better than mismatched base pairs.[59,60,61] These were to be combined with LNA residues, introduced via commercially available phosphoramidite building blocks.[62]

When selecting replacements for thymidine residues, we drew on the results of our recent combinatorial search on duplex-stabilizing substituents protruding into the major groove of duplex DNA.[63] A pyrenylbutyramidopropargyl ligand attached to the 5-position of 2′-deoxyuridine residues had been identified as the substituent giving the largest melting point increase. Thus far, the deoxyuridine residues carrying the substituent had to be coupled to fully assembled oligonucleotides on solid support via cross coupling of 2′-deoxy-5-iodouridine residues.[63] This procedure was unattractive for regular use in microarray syntheses. We therefore synthesized phosphoramidite **1** (Scheme 1), which allows for chain assembly via automated DNA synthesis without any unconventional steps. The synthesis of **1** started with coupling of pyrenylbutyric acid (**2**) to propargylamine (**3**). Amide **4** was then used in a Sonogashira coupling with 5′-protected 2′-deoxy-5-iodouridine **5**. The resulting alkynyl nucleoside **6** was then phosphitylated to give **1** in 66% overall yield.

We then tested to what extent the pyrenyldeoxyuridine residues act synergistically with molecular caps (Scheme 2). We chose a trimethoxystilbene cap for the 5′-terminus, readily introduced at the end of DNA syntheses via phosphoramidite **7**,[61] which is commercially available. The three-dimensional structure of a duplex capped by this 5′-substituent is known.[64] Stilbenes had previously been shown to be excellent

(41) (a) Nguyen, H.-K.; Fuornier, O.; Assaline, U.; Dupret, D.; Thuong, N. T. *Nucleic Acids Res.* **1999**, *27*, 1492−1498. (b) Nguyen, H.-K.; Bonfils, E.; Auffray, P.; Costaglioli, P.; Schmitt, P.; Asseline, U.; Durand, M.; Maurizot, J.-C.; Dupret, D.; Thuong, N.T. *Nucleic Acids Res.* **1998**, *26*, 4249−4258. (c) Nguyen, H.-K.; Auffray. P.; Asseline, U.; Dupret, D.; Thuong, N. T. *Nucleic Acids Res.* **1997**, *25*, 3059−3065.
(42) Fidanza, J. A.; McGall, G. H. *Nucleosides Nucleotides Nucleic Acids* **1999**, *18*, 1293−1295.
(43) (a) He, J.; Seela, F. *Nucleic Acids Res.* **2002**, *30*, 5485−5496. (b) Seela, F.; Becher, G. *Nucleic Acids Res.* **2001**, *29*, 2069−2078. (c) Seela, F.; Zulauf, M. *Helv. Chim. Acta* **1999**, *82*, 1878−1898.
(44) Nielsen, P. E. *Annu. Rev. Biophys. Biomol. Struct.* **1995**, *24*, 167−183.
(45) Uhlmann, E.; Peyman, A.; Breipohl, G.; Will, D. W. *Angew. Chem. Int Ed.* **1998**, *37*, 2797−2823.
(46) (a) Christensen, N. K.; Petersen, M.; Nielsen, P.; Jacobsen, J. P.; Olsen, C. E.; Wengel, J. *J. Am. Chem. Soc.* **1998**, *120*, 5458−5463. (b) Koshkin, A.A.; Singh, S. K.; Nielsen, P.; Rajwanshi, V. K.; Kumar, R.; Meldgaard, M.; Olsen, C. E.; Wengel, J. *Tetrahedron* **1998**, *54*, 3607−3630. (c) Obika, S.; Nanbu, D.; Hari, Y.; Andoh, J.I.; Morio, K.I.; Doi, T.; Imanishi, T. *Tetrahedron Lett.* **1998**, *39*, 5401−5404.
(47) Nielsen, K. E.; Singh, S. K.; Wengel, J.; Jacobsen, J. P. *Bioconjugate Chem.* **2000**, *11*, 228−238.
(48) Tolstrup, N.; Nielsen, P. S.; Kolberg, J. G.; Frankel, A. M.; Vissing, H.; Kauppinen, S. *Nucleic Acids Res.* **2003**, *31*, 3758−3762.
(49) (a) Gryaznov, S. M.; Chen, J.-K. *J. Am. Chem. Soc.* **1994**, *116*, 3143−3144. (b) Chen, J.-K.; Schultz, R. G.; Lloyd, D. H.; Gryaznov, S. M. *Nucleic Acids Res.* **1995**, *23*, 2661−2668. (c) Gryaznov, S. M.; Lloyd, D. H.; Chen, J.-H.; Schultz, R. G.; DeDionisio, L. A.; Ratmeyer, L.; Wilson, W. D. *Proc. Natl. Acad. Sci. U.S.A.* **1995**, *92*, 5798−5802.
(50) Linkletter, B. A.; Szabo, I. E.; Bruice, T. C. *J. Am. Chem. Soc.* **1999**, *121*, 3888−3896.
(51) Hendrix, C.; Rosemeyer, H.; De Bouvere, B.; Van Aerschot, A.; Seela, F.; Herdewijn, P. *Chem. Eur. J.* **1997**, *3*, 110−120.
(52) Freier, S. M.; Altmann, K. H. *Nucleic Acids Res.* **1997**, *25*, 4429−4443.
(53) Manoharan, M. *Biochim. Biophys. Acta* **1999**, *1489*, 117−130.
(54) Summerton, J. *Biochim. Biophys. Acta* **1999**, *1489*, 141−158.
(55) Richert, C.; Roughton, A. L.; Benner, S. A. *J. Am. Chem. Soc.* **1996**, *118*, 4518−4531.
(56) Benner, S. A.; Hutter, D. *Bioorg. Chem.* **2002**, *30*, 62−80.
(57) (a) Fodor, S. P. A.; Read, J. L.; Pirrung, M. C.; Stryer, L.; Lu, A. T.; Solas, D. *Science* **1991**, *251*, 767−773. (b) Pirrung, M. C. *Chem. Rev.* **1997**, *97*, 473−488. (c) Gao, X. L.; Gulari, E.; Zhou, X. C. *Biopolymers* **2004**, *73*, 579−596.
(58) Richert, C.; Grünefeld, P. *Synlett* **2007**, 1−18.
(59) Bleczinski, C. F.; Richert, C. *J. Am. Chem. Soc.* **1999**, *121*, 10889−10894.
(60) Narayanan, S.; Gall, J.; Richert, C. *Nucleic Acids Res.* **2004**, *32*, 2901−2911.
(61) Dogan, Z.; Paulini, R.; Rojas Stütz, J. A.; Narayanan, S.; Richert, C. *J. Am. Chem. Soc.* **2004**, *126*, 4762−4763.
(62) For reviews on LNAs, see: (a) Wengel, J. *Acc. Chem. Res.* **1999**, *32*, 301−310. (b) Jepsen, J. S.; Wengel, J. *Curr. Opin. Drug Discov. Dev.* **2004**, *7*, 188−194.
(63) Kottysch, T.; Ahlborn, C.; Brotzel, F.; Richert, C. *Chem. Eur. J.* **2004**, *10*, 4017−4028.

Scheme 1. Synthesis of Phosphoramidite **1**[a]

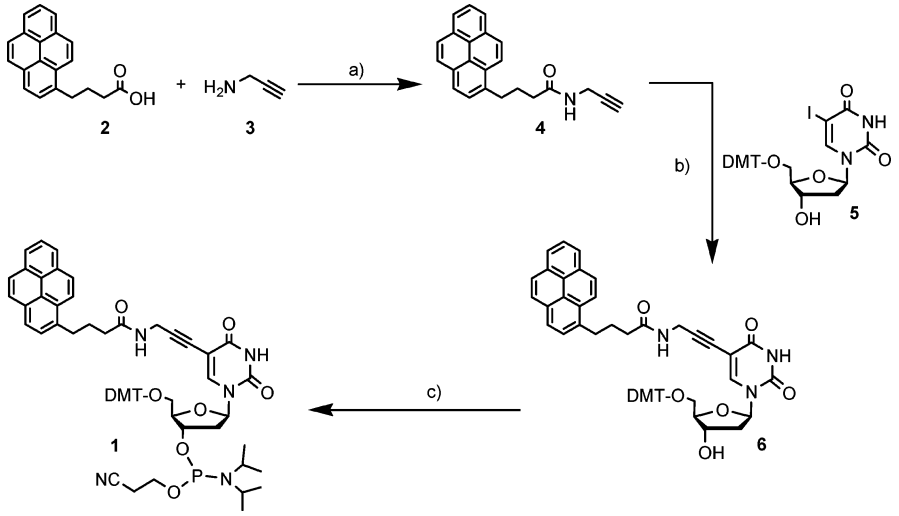

[a] Conditions: (a) HOBt, EDC, DMF, 76%; (b) $Pd(PPh_3)_4$, CuI, NEt_3, DMF, 92%; (c) $NCC_2H_4O-P(NiPr_2)Cl$, DIEA, CH_3CN, 95%.

Scheme 2. Synthesis of "Highly Decorated", Lysine-Terminated Oligonucleotide **AT2CapPyLNA** (**12**)[a]

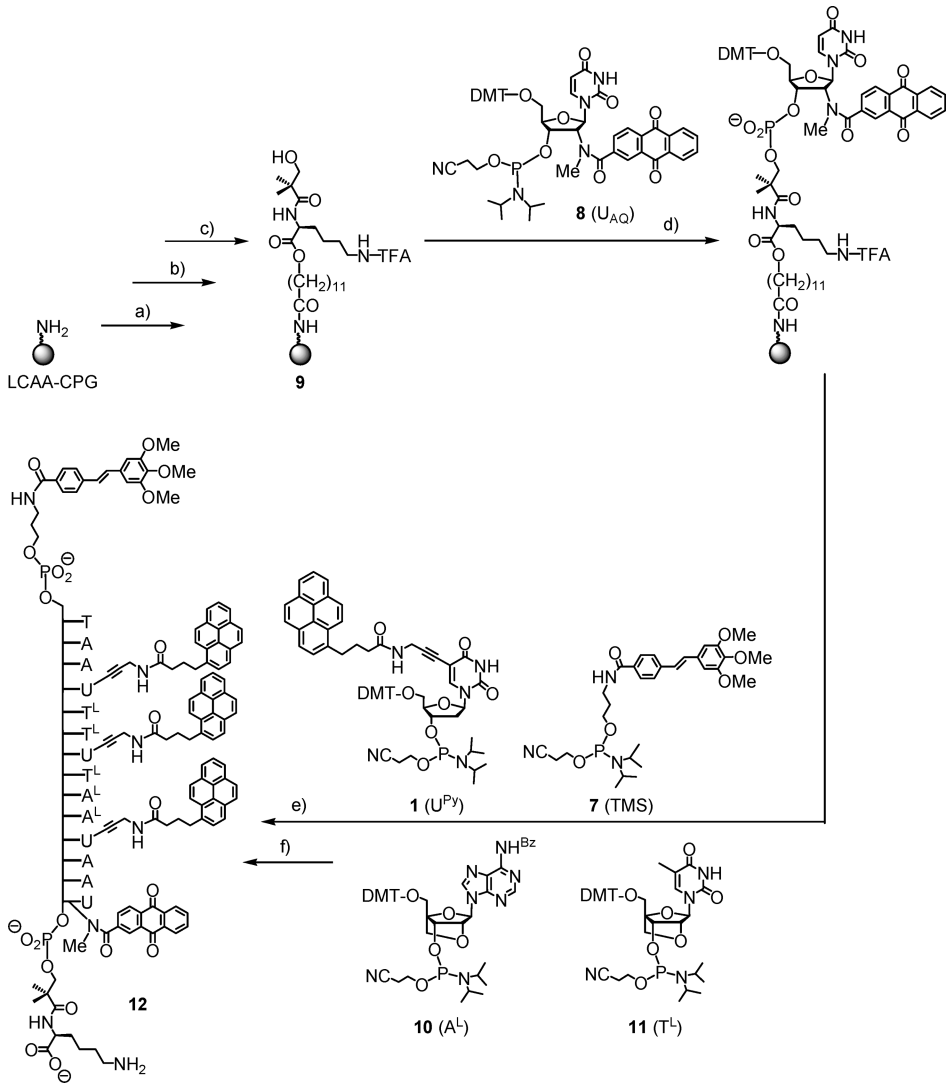

[a] Controlled pore glass **9**[67] was prepared as reported: (a) 1. 12-trityloxylauric acid, HBTU, HOBt, DIPEA, DMF, 2. TFA/CH_2Cl_2 (1:1); (b) 1. Boc-Lys(TFA)-OH, HBTU, HOBt, DIPEA, DMF, 2. TFA/CH_2Cl_2; (c) 1. 2,2-dimethyl-3-trityloxypropionic acid, HBTU, HOBt, DIPEA, DMF, 2. TFA/CH_2Cl_2; (d) tetrazole, CH_3CN, followed by oxidation and capping; (e) conventional DNA synthesis, including **1**, **7**, **10**, and **11**; (f) NH_4OH.

bridges for termini of duplexes.[65] Oligonucleotides with the trimethoxystilbene cap show excellent mismatch discrimination at the terminus, both in solution and on microarrays.[61] A cholic acid residue amide-linked to the 5′-terminus[59] was also tested

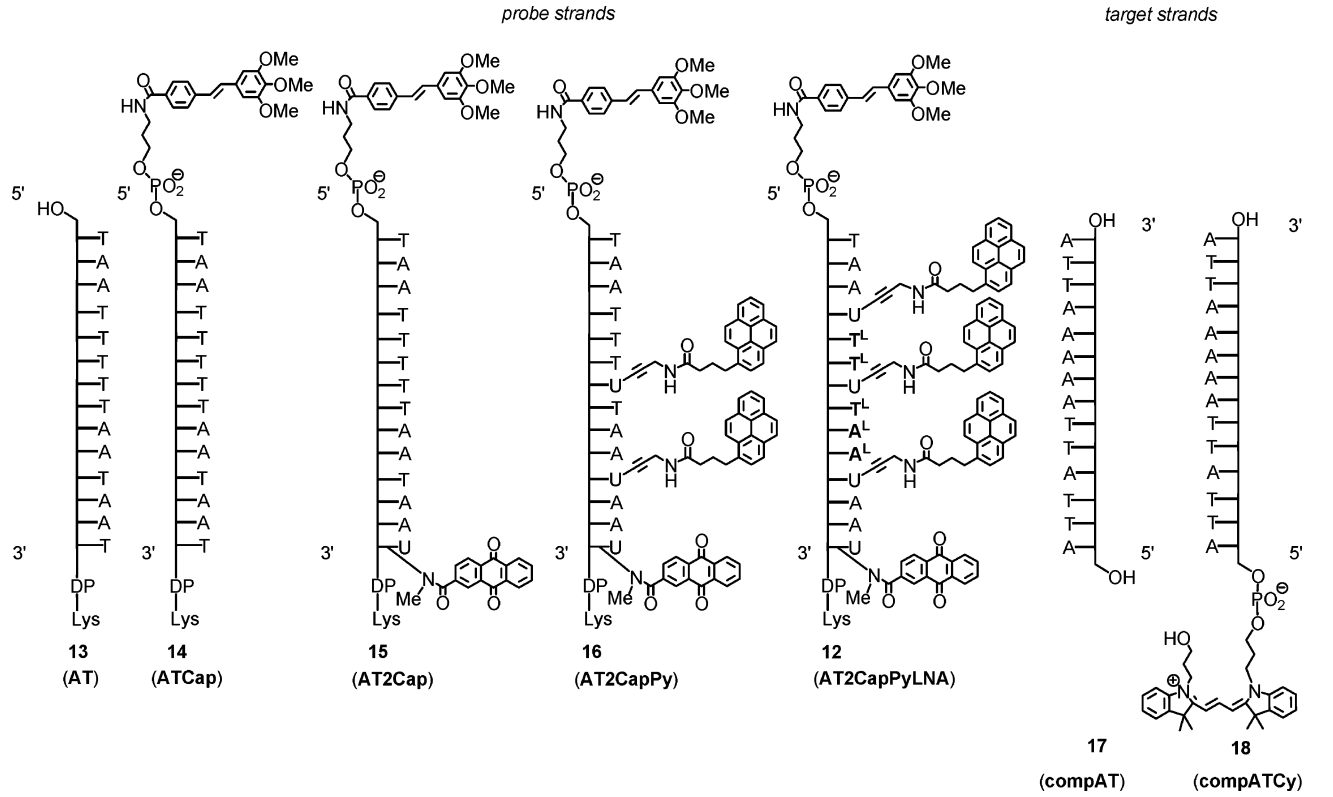

Figure 2. Oligonucleotides binding an all-A/T target sequence with an increasing number of duplex-stabilizing ligands or LNA residues. The T^L and A^L in **AT2CapPyLNA** (**12**) denote the LNA analogues of thymidine and deoxyadenosine residues, respectively; DP-Lys denotes the dimethylpropionic acid-lysine linker. See **AT2CapPyLNA** (**12**) in Scheme 2 for the structure of the 3′-terminus.

and gave similar results, both in solution and on microarrays, but was not pursued further, as it requires a 5′-terminal 5′-amino-2′,5′-dideoxynucleotide and amide-forming steps during solid-phase syntheses. A pyrenylmethylpyrrolidinol 5′-cap[60] produced oligonucleotides that were difficult to purify to homogeneity when additional lipophilic residues were incorporated.

For the 3′-terminus, a 2′-attached anthraquinonecarboxamido group (AQ) was chosen, which has recently been shown to increase duplex stability on DNA-microarrays.[66] This substituent is also known to induce satisfactory mismatch discrimination at the terminus.[60] The synthesis of the phosphoramidite **8** and its use as reagent for generating oligonucleotides with a linker for 3′-immobilization on aldehyde-bearing glass surfaces has been reported.[66] The lysine-terminated linker[67] has been used for microarrays previously.[68,61]

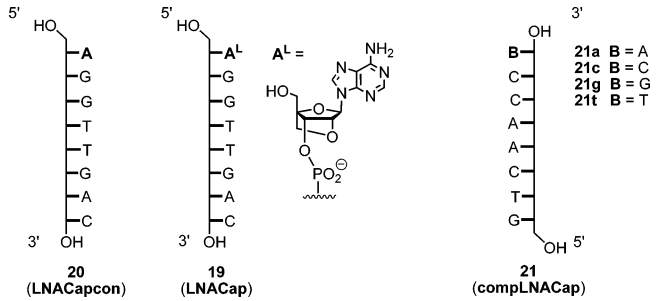

Figure 3. Oligonucleotides **LNACap** (**19**), **LNACapcon** (**20**), and **compLNACap** (**21**) used in melting curve experiments (compare Table 1).

Starting from linker-bearing controlled pore glass **9** (Scheme 2) the synthesis of oligonucleotide **AT2CapPyLNA** (**12**) was performed, using phosphoramidites **1**, **7**, **8** and LNA-phosphoramidites **10** and **11**, as well as the phosphoramidites of unmodified nucleosides (Scheme 2).[69] A series of oligonucleotides featuring only subsets of the duplex-stabilizing ligands [**AT** (**13**), **ATCap** (**14**), **AT2Cap** (**15**), and **AT2CapPy** (**16**)] was also prepared (Figure 2), using the analogous strategy but fewer nonstandard phosphoramidites. Further, the DNA target sequence fully complementary to **12**−**16**, namely **compAT**, 5′-ATTATTAAAAATTA-3′ (**17**) was prepared, together with its Cy-labeled analogue **compATCy**, 5′-Cy3-ATTATTAAAAATTA-3′ (**18**).

(64) Tuma, J.; Paulini, R.; Rojas Stütz, J. A.; Richert, C. *Biochemistry* **2004**, *43*, 15680−15687.
(65) Lewis, F. D.; Liu, X.; Wu, Y.; Miller, S. E.; Wasielewski, M. R.; Letsinger, R. L.; Sanishivili, R.; Joachimiak, A.; Tereshko, V.; Egli, M. *J. Am. Chem. Soc.* **1999**, *121*, 9905−9906.
(66) Al-Rawi, S.; Ahlborn, C.; Richert, C. *Org. Lett.* **2005**, *7*, 1569−1572.
(67) Schwope, I.; Bleczinski, C. F.; Richert, C. *J. Org. Chem.* **1999**, *64*, 4749−4761.
(68) Dombi, K.; Griesang, N.; Richert, C. *Synthesis* **2002**, 816−824.
(69) For the oligonucleotides, a short-hand naming system is being used in addition to the numbering to make the text easier-to-read. For example, **AT**, **ATCap**, **AT2Cap**, and **AT2CapPy** denote oligonucleotides of the all-A/T series without substituents, with one cap, two caps, and two caps plus pyrenyl substituents, respectively. Names starting with **GC** refer to compounds from the all-G/C series. The prefix **comp** stands for the complementary strand, and the endings **con**, **Cy**, and **LNA** refer to control compounds, cyanine dye-labeled compounds, and LNA-containing compounds, respectively. In the **GC** series, **Et** and **I** indicate the presence of ethylcytosine and inosine residues in the oligonucleotide with numbers indicating how many are found in the sequence. Strands with a mismatched nucleobase contain an ending highlighting this nucleobase, e.g., **compGC_A** for a complementary strand with a mismatched adenine residue. See the Supporting Information for a separate listing of the short-hand convention.
(70) Koshkin, A. A.; Singh, S. K.; Nielsen, P.; Rajwanshi, V. K.; Kumar, R.; Meldgaard, M.; Olsen, C. E.; Wengel, J. *Tetrahedron*, **1998**, *54*, 3607−3630.
(71) (a) Kaur, H.; Arora, A.; Wengel, J.; Maiti, S. *Biochemistry* **2006**, *45*, 7347−7355. (b) You, Y.; Moreira, B. G.; Behlke, M. A.; Owczarzy, R. *Nucleic Acids Res.* **2006**, *34*, e60.
(72) Reich, N. O.; Sweetnam, K. R. *Nucleic Acids Res.* **1994**, *22*, 2089−2093.

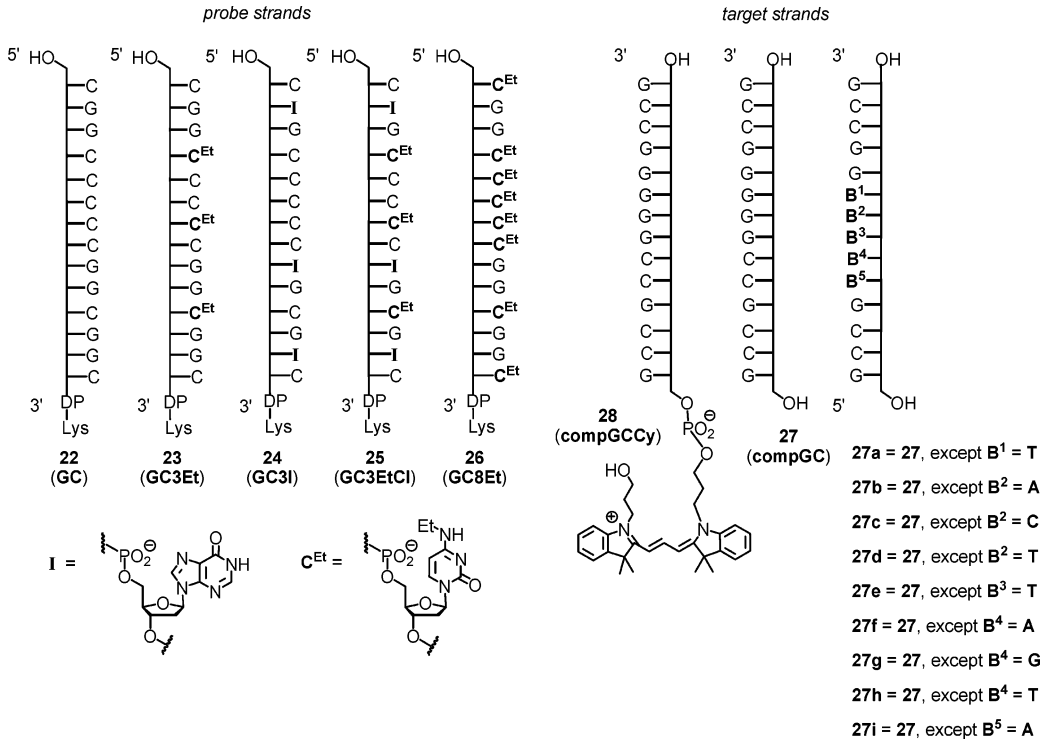

Figure 4. Oligonucleotides prepared with an all-G/C-sequence and different numbers of substituents. In the sequence, C^{Et} is indicating *N*-4-ethylcytidine and I indicates inosine residues.

Table 1. UV-Melting Points of Duplexes of Oligonucleotide **LNACap** (**19**) or **LNACapcon** (**20**) with Their Complementary Strand and Mismatch-Containing Derivatives of **compLNACap** (**21a**−**t**)

Duplex[a]: 5′-**Y**GGTTGAC-3′ **LNACap** (**19**) or **LNACapcon** (**20**)
3′-**B**CCAACTG-5′ **compLNACap** (**21a-t**)

		150 mM NH_4OAc			1 M NH_4OAc		
Y[b]	B	T_m (°C)[c]	ΔT_m (°C)[d]	hyperchr (%)[e]	T_m (°C)[c]	ΔT_m (°C)[d]	hyperchr (%)[e]
A	T	27.3 ± 0.4		20	35.7 ± 0.3		21
A	C	26.0 ± 0.6	−1.3	17	34.4 ± 0.5	−1.3	18
A	A	26.8 ± 0.7	−0.5	19	34.9 ± 0.7	−0.8	19
A	G	28.0 ± 0.6	0.7	23	36.5 ± 0.7	0.8	24
A^L	T	28.7 ± 0.5		18	37.1 ± 0.4		18
A^L	C	24.3 ± 0.7	−4.4	17	32.9 ± 0.6	−4.2	17
A^L	A	24.8 ± 0.4	−3.9	17	33.3 ± 0.5	−3.8	18
A^L	G	25.7 ± 0.6	−3.0	20	33.7 ± 0.5	−3.4	20

[a] Conditions: 1.5 μM strand concentration for each oligonucleotide, NH_4OAc-buffer, pH 7.0. [b] $\mathbf{A^L}$ denotes LNA A residue. [c] Average of four melting points ± standard deviation. [d] Difference of melting points according to fully complementary duplex. [e] Average of hyperchromicities (hyperchr) from 4 curves, measured at 260 nm.

Table 2. UV-Melting Points of Duplexes of **GC** (**22**) or **GC3Et** (**23**) and Target Strands with or without a Mismatched Nucleobase Opposite to or Next to a Modified Cytosine Residue

Duplex[a]: 5′-CGG**N**C C**N**C GG**N**GGC-DP-Lys3′ **GC** (**22**) or **GC3Et** (**23**)
3′-GCCGG**$B^1B^2B^3$**CCGCCG-5′ **compGC** (**27**, **27a-e**)

		150 mM NaCl			1 M NaCl		
N[b]	$B^1B^2B^3$	T_m (°C)[c]	ΔT_m (°C)[d]	hyperchr (%)[e]	T_m (°C)[c]	ΔT_m (°C)[d]	hyperchr (%)[e]
C	G**G**G	72.4 ± 0.4	-	14	75.8 ± 0.4		15
C	G**A**G	58.3 ± 0.8	−14.1	12	63.3 ± 0.4	−12.5	13
C	G**C**G	54.9 ± 0.4	−17.5	11	61.5 ± 0.3	−14.3	12
C	G**T**G	57.2 ± 0.7	−15.2	9	62.2 ± 0.2	−13.6	8
C	GG**T**	53.5 ± 0.8	−18.9	12	59.4 ± 0.4	−16.4	13
C	**T**GG	56.7 ± 0.5	−15.7	10	61.0 ± 0.1	−14.8	10
C^{Et}	G**G**G	63.1 ± 0.7	-	15	66.9 ± 0.4		18
C^{Et}	G**A**G	51.9 ± 0.9	−11.2	14	55.3 ± 0.3	−11.6	14
C^{Et}	G**C**G	47.6 ± 1.3	−15.5	12	53.7 ± 0.5	−13.2	12
C^{Et}	G**T**G	48.9 ± 0.8	−14.2	11	54.0 ± 0.5	−12.9	11
C^{Et}	GG**T**	45.1 ± 0.8	−18.0	11	49.7 ± 0.9	−17.2	11
C^{Et}	**T**GG	46.8 ± 1.0	−16.3	10	51.3 ± 0.7	−15.6	11

[a] Conditions: 1 μM strand concentration (each), salt concentration 150 mM NaCl, 10 mM sodium phosphate buffer (pH7) and 150 mM NaCl; 1 M NaCl, 10 mM sodium phosphate buffer (pH7) and 1 M NaCl. [b] C^{Et} denotes *N*-4-ethylcytidine [c] Average of four melting points ± SD. [d] ΔT_m = melting point difference with respect to the perfectly matched duplex. [e] Average of hyperchromicities (hyperchr) at 260 nm upon duplex dissociation from 4 curves.

Experiments were then performed to evaluate whether a molecular cap provides better base pairing fidelity at the terminus than an LNA residue. The results from a series of melting curve experiments with oligonucleotide **LNACap** (**19**) featuring a 5′-terminal LNA-nucleoside or unmodified control **LNACapcon** (**20**) with target strands **compLNACap** (**21a-t**) featuring a matched or mismatched nucleobase at their 3′-terminal position (Figure 3) showed very modest decreases in melting point for the mismatches. The same terminal mismatches in duplexes of 5′-TMS-**B**GGTTGAC-3′, where TMS is a trimethoxystilbene cap and **B** is A, C, G, or T give melting point depressions of between 6.5 and 23.4 °C, justifying the use of caps, rather than using LNA only. Further, the melting point increase for the fully complementary duplex is much greater for the TMS cap (up to +12.2 °C for an octamer)[61] than for a terminal LNA residue (Table 1). As a consequence, LNA nucleosides were only used in the interior of the sequence. For the pyrenyl-substituent at the 5-position of dU residues, satisfactory mismatch discrimination had been demonstrated previously,[63] and the same is true for the 3′-anthraquinone substituent.[60] For LNA oligonucleotides where the LNA residues are in the interior of the sequence, data on base pairing selectivity[70] and stabilizing effects are known from the literature.[71] These

Table 3. UV-Melting Points of Duplexes of **GC** (**22**) (control) or **GC3I** (**24**) and Target Strands with or without a Mismatched Nucleobase Directly Facing the Deoxyinosine Residue or Next to It

Duplex[a]: 5′-**CN**GCCCC C**N** G CG**N**C–DP-Lys-3′ **GC** (**22**) or **GC3I** (**24**)
3′-GCCGGGG **B^{3}B^{4}B^5**GCCG-5′ **compGC** (**27**, **27e-i**)

		150 mM NaCl			1 M NaCl		
N[b]	B^{3}B^{4}B^5	T_m (°C)[c]	ΔT_m (°C)[d]	hyperchr (%)[e]	T_m (°C)[c]	ΔT_m (°C)[d]	hyperchr (%)[e]
G	GCC	72.4 ± 0.4		14	75.8 ± 0.4		15
G	G**A**C	63.5 ± 0.3	−8.9	14	66.9 ± 0.3	−8.9	14
G	G**G**C	61.9 ± 0.2	−10.5	14	65.1 ± 0.3	−10.7	13
G	G**T**C	62.9 ± 0.6	−9.5	14	66.8 ± 0.3	−9.0	14
G	GC**A**	66.3 ± 0.5	−6.1	14	70.3 ± 0.4	−5.5	15
G	**T**CC	54.2 ± 0.4	−18.2	11	59.2 ± 0.7	−16.6	13
I	GCC	59.5 ± 0.8		13	64.0 ± 0.3		16
I	G**A**C	58.9 ± 0.3	−0.6	15	64.3 ± 0.3	+ 0.3	15
I	G**G**C	53.2 ± 0.2	−6.3	15	57.0 ± 0.3	−7.0	16
I	G**T**C	54.4 ± 0.4	−5.1	15	58.8 ± 0.3	−5.2	16
I	GC**A**	53.8 ± 0.4	−5.7	14	58.6 ± 0.5	−5.4	15
I	**T**CC	38.3 ± 0.6	−21.2	10	45.0 ± 0.7	−19.0	12

[a] Conditions: 1 μM strand concentration, salt concentration 150 mM NaCl, 10 mM sodium phosphate buffer (pH7) and 150 mM NaCl; 1 M NaCl, 10 mM sodium phosphate buffer (pH7) and 1 M NaCl. [b] I denotes deoxyinosine residue. [c] Average of four melting points ± SD. [d] ΔT_m = melting point difference with respect to the perfectly matched duplex. [e] Average of hyperchromicities (hyperchr) at 260 nm upon duplex dissociation from 4 curves.

are generally more favorable than those of the corresponding values for unmodified DNA.

Next, approaches for reducing the thermal stability of the all-G/C counterpart of AT (**13**) without loss of base-pairing fidelity was tested. For this, the tetradecamers shown in Figure 4 were synthesized and employed in UV-melting experiments. They include control compound **GC** (**22**) with unmodified nucleobases and sequences with deoxyinosine[72] and 2′-deoxy-*N*4-ethylcytidine residues[41] replacing deoxyguanosine and deoxycytidine residues, respectively. The sequences **GC** (**22**), **GC3Et** (**23**), **GC3I** (**24**), **GC3EtCI** (**25**), and **GC8Et** (**26**) feature the same order of purines and pyrimidines as in the all-A/T sequences **AT2CapPyLNA** (**12**), **AT** (**13**), **ATCap** (**14**), **AT2Cap** (**15**), and **AT2CapPy** (**16**). Inosine can form only two hydrogen bonds, compared to three for guanine, and the ethyl chain at the *N*4-position reduces base-pair stability based on an entropic effect (only one of the two conformers is capable of pairing with G). The synthesis of compounds **GC** (**22**), **GC3Et** (**23**), **GC3I** (**24**), **GC3EtCI** (**25**), and **GC8Et** (**26**) started from linker-bearing cpg **9** (Scheme 2), so that strands suitable for immobilization on microarray surfaces were obtained. The fully complementary target strand **compGC** 5′-GCCGCCGGGGGC-CG-3′ (**27**), its fluorophore-labeled counterpart **compGCCy** 5′-Cy3-GCCGCCGGGGGCCG-3′ (**28**), and mismatch-containing derivatives (**27a**−**i**) were also prepared via conventional chain-assembly strategies.

To test the effect of the base modification on base pairing fidelity, melting curves with complementary strands containing a mismatched nucleobase directly opposite the inosine/*N*4-ethylcytosine or immediately next to the base pair it forms were performed. The results are compiled in Tables 2 and 3. It can be discerned that an *N*4-ethylcytosine residue retains the base pairing specificity of cytosine, with fairly similar drops in melting point for mismatch-containing duplexes of at least 11.2 °C. The same cannot be said of inosine as replacement for guanine. Particularly, a mismatched adenine facing the inosine in duplex, **GC3I**:**compGC_A** (**24** : **27f**) leads to an unusually stable duplex, whose melting point rivals that of the perfectly matched counterpart. As a consequence, oligonucleotides **GC3I** (**24**) and **GC3EtCI** (**25**) (Figure 4) were not used for further experiments, even though the latter had shown the required drop in melting point for the duplex with its complementary target strand (the T_m of duplex **GC3EtCI**:**compGC** (**25**:**27**) is 47.8 ± 0.8 °C at 150 mM NaCl and 52.9 ± 0.6 °C at 1 M NaCl).

The next focus of our study was on measuring the extent to which the modifications introduced to the all-A/T sequence motif and the all-G/C sequence motif produced isostable DNA.

Table 4. UV-Melting Points of Duplexes of **AT** (**13**), **ATCap** (**14**), **AT2Cap** (**15**), **AT2CapPy** (**16**), **AT2CapPyLNA** (**12**) and **GC** (**22**), **GC3Et** (**23**), **GC8Et** (**26**) with Fully Complementary Target Strands

salt oligonucleotide sequence[a,b]	target strand[a,b]	T_m (°C)[c]	ΔT_m (°C)[d]	hyperchr (%)[e]
150 mM NaCl				
TAATTTTTAATAAT (**13**)	ATTATTAAAAATTA (**17**)	31.4 ± 0.4		35
TMS-TAATTTTTAATAAT (**14**)		37.4 ± 0.5	6.0	36
TMS-TAATTTTTAATAA**U$_{AQ}$** (**15**)		41.9 ± 0.4	10.5	33
TMS-TAATTT**U^{Py}**TAA**U^{Py}**AA**U$_{AQ}$** (**16**)		44.9 ± 0.3	13.5	26
TMS-TAA**U^{Py}T^{L}T^{L}U^{Py}T^{L}A^{L}A^{L}U^{Py}**AA**U$_{AQ}$** (**12**)		54.9 ± 0.3	23.5	26
CGGCCCCCGGCGGC (**22**)	GCCGCCGGGGGCCG (**27**)	72.4 ± 0.4		14
CGG**C^{Et}**CCC**C^{Et}**CGG**C^{Et}**GGC (**23**)		63.1 ± 0.7	−9.3	15
C^{Et}GG**C^{Et}C^{Et}C^{Et}C^{Et}C^{Et}**GG**C^{Et}**GG**C^{Et}** (**26**)		48.3 ± 0.4	−24.1	15
1 M NaCl				
TAATTTTTAATAAT (**13**)	ATTATTAAAAATTA (**17**)	40.7 ± 0.6		36
TMS-TAATTTTTAATAAT (**14**)		46.1 ± 0.5	5.4	36
TMS-TAATTTTTAATAA**U$_{AQ}$** (**15**)		50.3 ± 0.5	9.6	32
TMS-TAATTT**U^{Py}**TAA**U^{Py}**AA**U$_{AQ}$** (**16**)		51.6 ± 0.3	10.9	25
TMS-TAA**U^{Py}T^{L}T^{L}U^{Py}T^{L}A^{L}A^{L}U^{Py}**AA**U$_{AQ}$** (**12**)		56.7 ± 0.3	16.0	26
CGGCCCCCGGCGGC (**22**)	GCCGCCGGGGGCCG (**27**)	75.8 ± 0.4		15
CGG**C^{Et}**CCC**C^{Et}**CGG**C^{Et}**GGC (**23**)		66.9 ± 0.4	−8.9	18
C^{Et}GG**C^{Et}C^{Et}C^{Et}C^{Et}C^{Et}**GG**C^{Et}**GG**C^{Et}** (**26**)		48.4 ± 0.5	−27.8	14

[a] Conditions: 1 μM strand concentration, salt concentration at 150 mM NaCl, 10 mM sodium phosphate buffer, pH 7, 150 mM NaCl at 1 M NaCl, 10 mM sodium phosphate buffer, pH 7, and 1 M NaCl. [b] Sequences are given from 5′- to 3′-terminus; **TMS** denotes a trimethocystilbene cap, **U$_{AQ}$** denotes deoxyuridine with an anthraquinone cap; **U^{Py}** denotes deoxyuridine with a pyrenylbutyramidopropargyl ligand, **T^{L}** and **A^{L}** denote LNA residues, and **C^{Et}** denotes *N*-4-ethyl-2′-deoxycytidine. See Figures 2 and 4 for structures. [c] Average of four melting points ± SD. [d] ΔT_m = melting point difference with respect to the unmodified duplex. [e] Average of hyperchromicities (hyperchr) at 260 nm upon duplex dissociation from 4 curves.

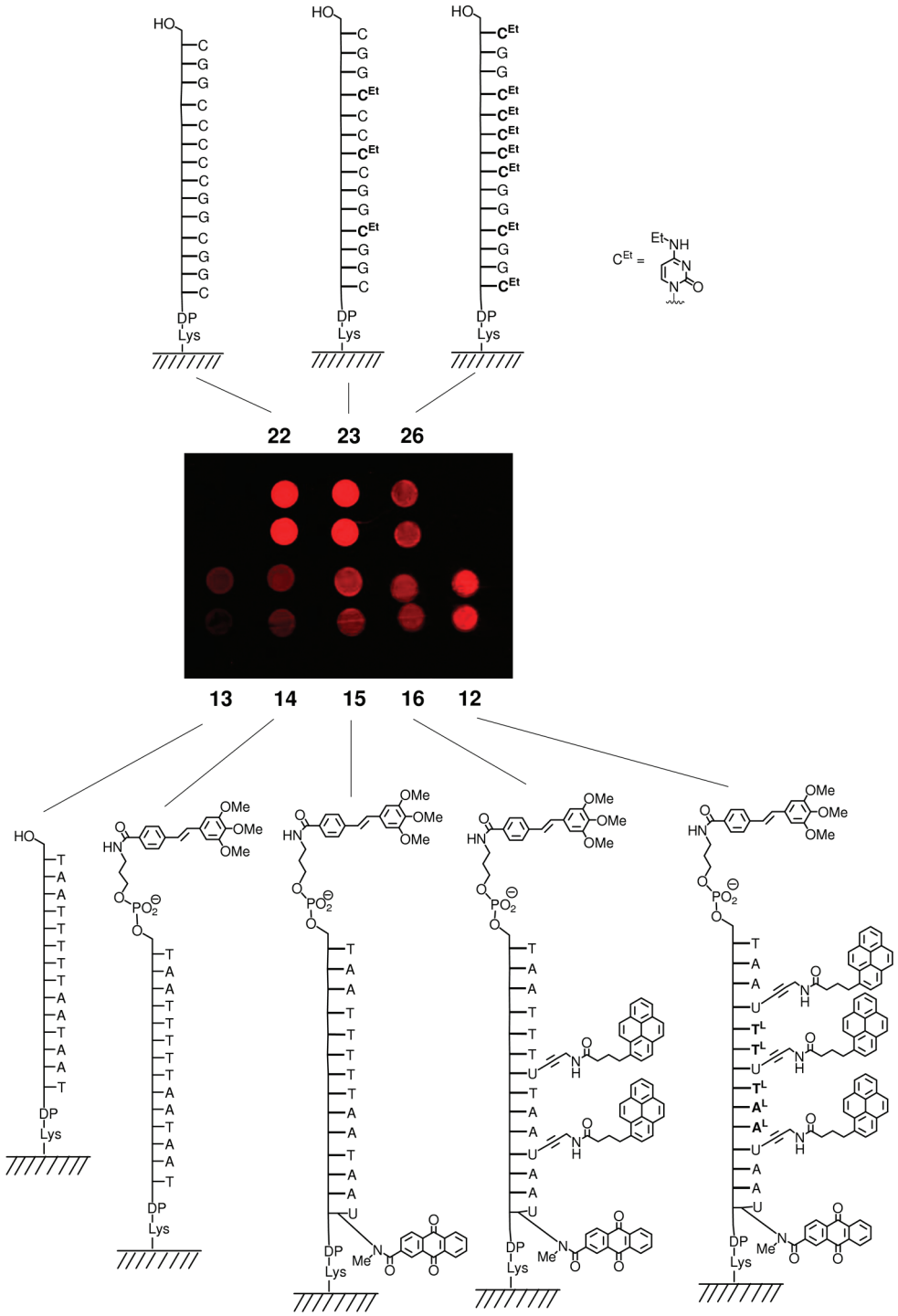

Figure 5. Fluorescence image of a microarray with low-density spots after hybridization and washing. Sequences of immobilized oligonucleotides are given above and below. Each oligonucleotide was immobilized in duplicate, with spots vertically above each other to demonstrate reproducibility, using spotting solutions containing 10 μM DNA, 2 × SSC, 0.2% SDS. The resulting spot size is approximately 2 mm. Hybridization was performed with a solution containing equimolar amounts of target oligonucleotides **compATCy** (**18**, 5′-Cy3-ATTATTAAAAATTA-3′) and **compGCCy** (**28**, 5′-Cy3-GCCGC-CGGGGGCCG-3′) at 10 μM each, in 0.1 M MES buffer, pH 6.3, for 1 h at 48 °C.

First, duplex stabilities were measured in homogeneous solution, using equimolar amounts of **AT2CapPyLNA** (**12**), **AT** (**13**), **ATCap** (**14**), **AT2Cap** (**15**), **AT2CapPy** (**16**), or **GC** (**22**), **GC3Et** (**23**), **GC8Et** (**26**), and target strands **compAT** (**17**) or **compGC** (**27**) (Table 4). Of the all-A/T sequences with decorating substituents only (**AT2CapPy**:**compAT**, **16**:**17**) brought the melting point within the range of that for the all-G/C motif with *N*4-ethylcytosines throughout (**GC8Et**:**compGC**, **26**:**27**). At 150 mM NaCl, the former duplex melted 3.4 °C below the latter; at 1 M salt, its melting point was 3.2 °C above that of the latter (Table 4). Incorporating five LNA residues on top of the duplex-stabilizing ligands (oligonucleotide **AT2CapPyLNA**, **12**), raised the melting point for the duplex with all-A/T target **compAT** (**17**) by another 5.1−10 °C, so that the goal of isostable duplexes was in fact exceeded, producing duplexes for an all-A/T motif that meet well above that for the tuned-down all-G/C counterpart **GC8Et**:**compGC** (**26**:**27**).

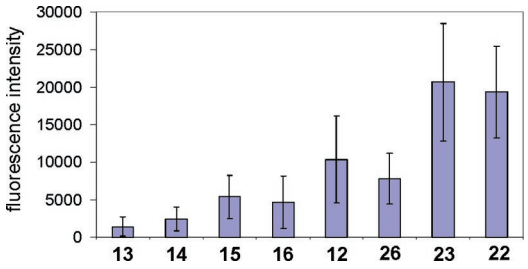

Figure 6. Fluorescence intensities generated through integration of the spot intensities of the type of image shown in Figure 5. The columns represent the mean of the two spots each from five independent arrays displaying the hybridization probe whose compound number is given below each bar. The short-hand codes are: **AT** (**13**), **ATCap** (**14**), **AT2Cap** (**15**), **AT2CapPy** (**16**), **AT2CapPyLNA** (**12**), **GC8Et** (**26**), **GC3Et** (**23**), and **GC** (**22**).

Our study thus showed that a decorated duplex based exclusively on T:A and A:T base pairs can have a higher thermal stability than the corresponding duplex containing only G:C and C^{Et}:G base pairs (Table 4). Furthermore, it is feasible to adjust target affinities stepwise by an increasing number of substituents introduced in the probe strands.

We then turned to microarray-based experiments. The oligonucleotide probes with their 3′-terminal lysine residue were covalently immobilized on aldehyde-coated glass slides using an optimized version of a known procedure[68] involving Schiff base formation, reduction, and capping of the remaining aldehyde groups (Scheme S1, Supporting Information). The first series of experiments involved manual microarray generation with a micropipette. Each oligonucleotide was spotted in duplicate, and the remaining surface was subsequently coated with a triethyleneglycol methyl ether terminating in an amino group.[68] A detailed study was performed to optimize the conditions for hybridizing to target strands **compATCy** (**18**) and **compGCCy** (**28**), including variation of the salt content, temperature, incubation time, and washing procedure. Further, control experiments with Cy3- and Cy5-labeled target strands were performed that confirmed the absence of detectable cross-hybridization between the target strands for the two different sequence motifs (all-A/T and all-G/C). The final experiments were performed with target strands featuring the *same* label (namely cyanine dye Cy3) to avoid a bias introduced by different fluorescence properties of the labels.

Figure 5 shows a typical fluorescence image of a microarray displaying probe strands **AT2CapPyLNA** (**12**), **AT** (**13**), **ATCap** (**14**), **AT2Cap** (**15**), **AT2CapPy** (**16**) and **GC** (**22**), **GC3Et** (**23**), **GC8Et** (**26**) after hybridization at 48 °C and washing at 48 and then 25 °C. The microarray assay was performed five times under the same conditions. The aggregate results from the quantitative fluorescence analyses are compiled in Figure 6. At the target strand concentration chosen (10 μM each), the signal for spots with the most strongly binding probe strands **GC** (**22**) and **GC3Et** (**23**) was near saturation. (The saturation signal level had also been independently confirmed in a series of microarray experiments involving probe strands **AT** (**13**) and **GC** (**22**) and from target strands **compATCy** (**18**) and **compGCCy** (**28**) (from 0.01 to 80 μM), see Figure S1, Supporting Information). More importantly, the most strongly enforced all-A/T strand (**AT2CapPyLNA**, **12**) bound more of its target (**compATCy**, **18**) than the most "tuned-down" version of the all-G/C sequence (**GC8Et**, **26**) bound its corresponding all-G/C target strand (**compGCCy**, **28**). This confirmed the observation from the in-solution experiments that duplex stability can be tuned beyond isostability. As expected, target affinity increased with an increasing number of duplex-stabilizing substituents, though **AT2CapPy** (**16**) bound slightly less of its target strand than **AT2Cap** (**15**) lacking the pyrenyl residues. This effect is not significant, however, considering the experimental error.

High fidelity multiplex detection of DNA on microarrays requires well chosen hybridization and washing conditions,[73] and predicting hybridization results has remained challenging thus far.[74] We therefore tested to what extent the fluorescence intensities measured agreed with theoretical binding curves, predicted with the computer program ChipCheck.[75,35] ChipCheck employs ΔH and ΔS values for predicting duplex formation. For the current duplexes involving modified strands, enthalpy and entropy of duplex formation were calculated from melting curves using MeltWin 3.0[76] (see Table S1, Supporting Information). The resulting theoretical binding curves in the temperature range 0−100 °C are shown in Figure 7. All input parameters for the ChipCheck simulation were those of the microarray experiment (30 μL hybridization solution, 10 μM target strand, 2.5 mm^2 spot size), with an estimated probe density of 10^{11} molecules/cm,[2,40] that is, 4×10^{-15} mol probes/spot.

The position of the curves in Figure 7 reflects the order of melting points (compare Table 4), with similar cooperativity for the individual transitions. The experimental values for each probe strand on the microarray spots (percent of the fluorescence signal at saturation) were entered as large symbols. Excellent agreement between calculated and experimental values was observed for the more tightly binding probe strands, down to the duplexes **AT2CapPyLNA**:**compAT** (**12**:**17**) and **GC8Et**:**compGC** (**26**:**27**), whose melting points are close to the temperature at which the microarray experiment was performed (48 °C). For duplexes with lower melting points, the experimental signal was stronger than predicted, suggesting a certain level of unspecific binding on the surface, probably due to the unoptimized surface chemistry of our custom-made microarrays.

Finally, a series of exploratory assays were performed with high-density microarrays. These involved the same immobilization method, but the spotting was performed by a robot suitable for producing high spot densities. The sequences of the oligonucleotides used, a representative fluorescence image after hybridization with the target strands and washing, and the integration of the fluorescence intensity for two different target concentrations are shown in Figure 8.

Again, the fluorescence intensities (Figure 8c/d) show that the affinity of the most strongly enforced oligonucleotide **AT2CapPyLNA** (**12**) for its all-A/T target **compATCy** (**18**) is in the same range as that of the tuned-down oligonucleotide probes **GC3Et** (**23**) and **GC8Et** (**26**) for their all-G/C target **compGCCy** (**28**), as required for a microarray with (roughly) isostable DNA. Further, an increasing number of duplex-stabilizing ligands was again found to lead to a stepwise increase in duplex stability for the all-A/T motif, while the introduction

(73) Han, T.; Melvin, C. D.; Shi, L. M.; Branham, W. S.; Moland, C. L.; Pine, P. S.; Thompson, K. L.; Fuscoe, J. C. *BMC Bioinformatics* **2006**, *7*, S17.
(74) Pozhitkov, A.; Noble, P. A.; Domazet-Loso, T.; Nolte, A. W.; Sonnenberg, R.; Staehler, P.; Beier, M.; Tautz, D. *Nucleic Acids Res.* **2006**, *34*, e66.
(75) Siegmund, K.; Steiner, U. E.; Richert, C. *J. Chem. Inf. Comput. Sci.* **2003**, *43*, 2153−2162.
(76) McDowell, J. A.; Turner, D. H. *Biochemistry* **1996**, *35*, 14077−14089.

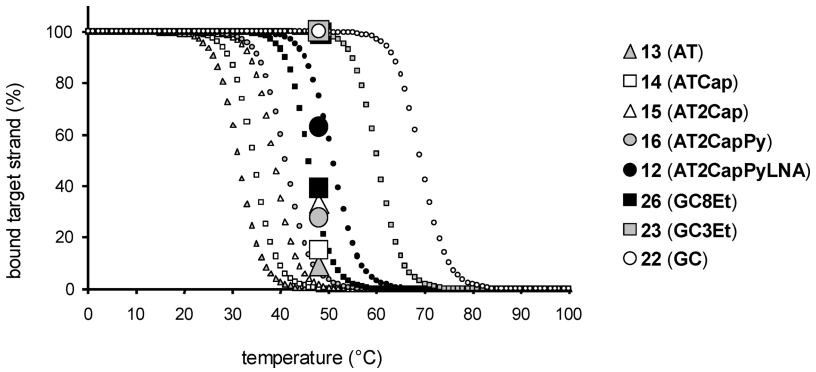

Figure 7. Binding curves for target strands **compAT** (**17**) and **compGC** (**27**), hybridizing to the probe strands listed in the legend on the right-hand side on microarray spots of 2.5 mm^2 size, as calculated with the computer program ChipCheck. Values from experimental data, obtained from fluorescence readings in microarray experiments with the same probe strands and labeled target strands **compATCy** (**18**) and **compGCCy** (**28**) (compare Figures 2 and 4) are entered at the hybridization temperature (48 °C) as large symbols. See Table 4 for sequences.

of ethylcytosine residues induces the necessary reduction in target affinity of the probes of the all-G/C motif. The agreement between predicted and observed binding was even better than for the low-density microarray (see Figure S2, Supporting Information).

Discussion

Besides technical issues, such as further reducing the background on microarrays, the current results open up questions regarding the concept of high fidelity DNA microarrays and its limitation. Fundamentally, the fidelity of molecular recognition should only be limited by the intrinsic binding energy,[77] offered by the nucleotides of the target strand. In natural DNA, the complexes formed between probe strands and target strands are fairly open. Compared to the active site of polymerases and kinases,[78−80] where a recognition from either π-surface and most of the hydrogen-bonding edges are realized, the extent to which a target strand is recognized in DNA duplexes is limited. If nature had had a need for maximum fidelity, rather than a compromise between fidelity, accessibility, and kinetic lability, duplexes with more fully engulfed nucleobases could certainly have been evolved. To what extent this compromise can be changed toward isostable DNA through chemical modifications, without affecting other physicochemical properties of DNA unfavorably, is not immediately clear, though.

It is therefore interesting to ask what type of chemical modification proved suitable for generating isostable DNA in our study and which did not. All successful modifications employed here are enforcing the duplex by bridging, by reducing its flexibility, or by filling up what would otherwise be a larger groove. The caps bridge the termini, thereby reducing fraying. The pyrenyl moieties attached via alkynyl linkers to the 5-position of deoxyuridines can be expected to intercalate,[63] again stiffening the duplex structure[81] both through bridging and through reduced dynamics along the helix axis. The ethyl substituents at position 4 of the cytosines will be located in the

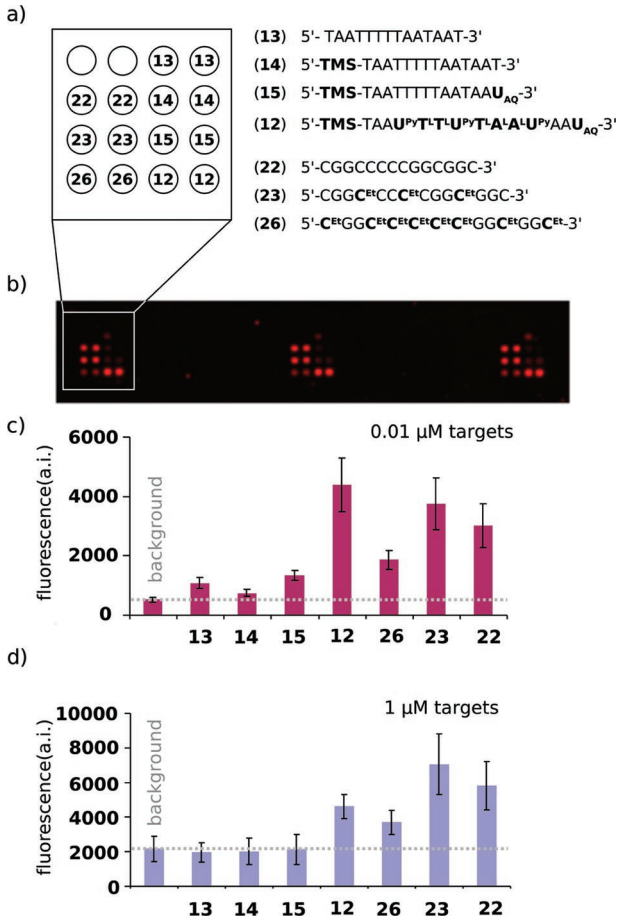

Figure 8. Results of microarray experiments with a high-density pattern of spots. (a) Pattern spotted in individual areas of the microarray. The numbers on the spots correspond to the sequences given on the right-hand side. Spotting solutions containing 10 μM DNA, 2 × SSC buffer, 0.2% SDS. Each compound was spotted twice to demonstrate reproducibility. (b) Fluorescence image of a section of the microarray featuring three spotting patterns after hybridization and washing. The spot size is approximately 80 μm in diameter. Hybridization was performed with a solution containing target strands oligonucleotide **compATCy** (**18**, 5′-Cy3-ATTATTAAAAATTA-3′) and **compGCCy** (**28**, 5′-Cy3-GCCGCCGGGGGCCG-3′), 0.01 μM each, in 2 × SSC, 0.2% SDS for 1 h at 48 °C. (c and d) Fluorescence intensities, as obtained through integration over areas of 80 μm diameter of individual spots, the values are the means of 16 patterns on one chip. Error bars show the standard deviation: (c) incubation with 0.01 μM target strands **compATCy** (**18**) and **compGCCy** (**28**); (d) incubation with 1 μM target strands.

(77) For the concept of intrinsic binding energy and its limits, see: Fersht, A. *Enzyme structure and mechanism*, 2nd ed.; W. H. Freeman: New York, 1985; pp 303; 348−350.
(78) Doublie, S.; Tabor, S.; Long, A. M.; Richardson, C. C.; Ellenberger, T. *Nature* **1998**, *391*, 251−258.
(79) For a review, see: Rothwell, P. J.; Waksman, G. *Adv. Protein Chem.* **2005**, *71*, 401−440.
(80) Bellinzoni, M.; Haouz, A.; Grana, M.; Munier-Lehmann, H.; Shepard, W.; Alzari, P. M. *Protein Sci.* **2006**, *15*, 1489−1493.
(81) (a) Lerman, L. S. *J. Mol. Biol.* **1961**, *3*, 18−30. (b) Saenger, W. *Principles of Nucleic Acid Structure* Springer, New York: 1984, p. 350.

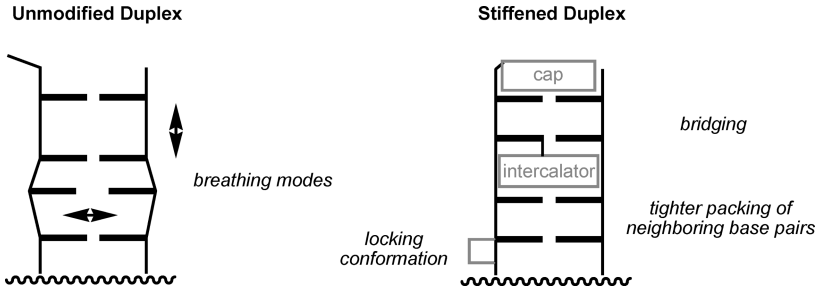

Figure 9. Cartoon highlighting differences in conformational flexibility in a natural duplex and a duplex involving a decorated nucleic acid probe. Compared to its unmodified counterpart the decorated duplex is expected to show a reduced propensity to form alternative, mismatched structures. Alternative structures may also be less well stabilized by caps, less well bridged by intercalators, and less well accommodating conformational locks.

major groove, where they take up some of the space otherwise filled by solvent. Finally, the methoxy locks of the LNA residues linking 2′- and 4′-position reduce the conformational flexibility of the deoxyriboses, again creating a stiffer structure[82] and increasing the number of contacts within the duplex.[83] Inosine, on the other hand, the only modification that failed to uphold base-pairing fidelity, is smaller than the guanine it replaces, leaving behind a hole that can be filled in a number of different ways, most of which open up ways for alternative base pairs that compete with the desired complex. Neither of the structures tested in our quest for high fidelity probes, which includes the current results and those of earlier studies,[59,61,63,60,84] was successful as a fidelity-enhancing element unless it created a larger structure than that of natural DNA. Apparently, the fewer alternative conformations are accessible and the more extensive the number of contacts with the target strands, the more scarce the number of alternative base-pairing arrangements, and the more likely that a high fidelity probe is being generated that binds only the fully complementary strand. A single accessible conformation with exquisitely sculptured surface that fits a single sequence in DNA structure space is the ultimate realization in this scenario (Figure 9, above).

To what extent do alternative structures that have been explored as hybridization probes on microarrays fit into this picture? Peptide nucleic acids (PNAs), for example, have been tested as probes, but have been found to be less uniform or less predictable in their hybridization properties than DNA.[85,86] PNA has high affinity for target strands because its nonionic backbone is not electrostatically repelled by the target strand. It features an acyclic backbone, though, for which more conformations are accessible than those found for DNA. In this more open structure, alternative complexes can form more readily. The lack of repulsion between like charges in the backbone also encourages backfolding of the PNA chains, a property they share with polypeptide chains, a class of biopolymers known for their ability to form diverse folded structures.[87] Other nonionic nucleic acid analogues also show a propensity to fold back onto themselves,[55] making them problematic for high fidelity recognition of target strands from a diverse set of sequences by a single, specific type of molecular interactions. The decorated nucleic acids presented here not only avoid a pruning of the backbone, they also have very few additional hydrogen-bonding sites. Instead, they feature substituents whose shape complementarity and effect on stiffness enforce specific molecular recognition without attracting alternative base-pairing arrangements, and the like charges of their phosphodiester anions help to reduce back-folding and aggregation.

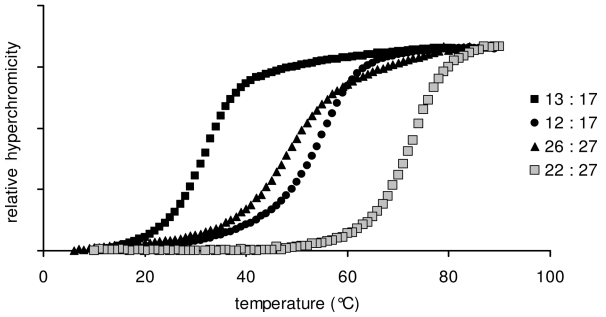

Figure 10. Overlay of UV-melting curves of duplexes without and with adjusted base-pairing strength. The duplexes of the all-A/T and all-G/C sequence motif without chemical modifications (**13**:**17** and **22**:**27**, respectively) are shown together with the curves of the most strongly modified versions of either sequence motif (**12**:**17** and **26**:**27**). Relative, rather than absolute, hyperchromicity was plotted to more easily judge how similar the cooperativity of the transitions is.

We would like to emphasize that our approach for adjusting duplex stability can be applied directly to existing platforms for microarray generation, including those involving photolithographic syntheses, since all building blocks employed are phosphoramidites. Further, it is clear from the extensive literature data on base-pairing fidelity at the terminus and the results for LNA residues at the terminus presented in Table 1 that the same effect cannot be achieved with LNAs alone. Still, it is important to ask to what extent ideal binding curves have been achieved with the chemical approach presented here. Figure 10 shows an overlay of the melting curves of the unmodified and most heavily modified duplexes of both the all-A/T and the all-G/C sequence motif. It can be discerned that the cooperativity of the melting transitions has not suffered from the covalent modifications introduced. Cooperative transitions are necessary for achieving high fidelity, as broad transitions favor situations where mismatched duplexes are partially formed while perfectly matched duplexes are still not fully formed at a given temperature. The results obtained on microarrays further confirm that equilibrium binding data obtained in solution are useful predictors for detection on chip surfaces, despite the fact that washing steps with the potential to bias those equilibria

(82) Other conformationally restricted DNA analogues exist; see, for example: (a) Renneberg, D.; Leumann, C. J. *J. Am. Chem. Soc.* **2002**, *124*, 5993−6002. (b) Steffens, R.; Leumann, C. J. *J. Am. Chem. Soc.* **1997**, *119*, 11548−11549.
(83) Egli, M.; Minasov, G.; Teplova, M.; Kumar, R.; Wengel, J. *Chem. Commun.* **2001**, 651−652.
(84) Connors, W. H.; Narayanan, S.; Kryatova, O. P.; Richert, C. *Org. Lett.* **2003**, *5*, 247−250.
(85) Igloi, G. L. *Proc. Natl. Acad. Sci. U.S.A.* **1998**, *95*, 8562−8567.
(86) Weiler, J.; Gausepohl, H.; Hauser, N.; Jensen, O. N.; Hoheisel, J. D. *Nucleic Acids Res.* **1997**, *25*, 2792−2799.
(87) Branden, C.; Tooze, J. Introduction to Protein Structure, 2nd ed.; Garland: New York, 1999.

through different dissociation kinetics are involved. Our results were obtained with short incubation times, suggesting that the added substituents of the decorated probes do not slow down the kinetics of duplex formation to a point that requires adjusting of protocols.

One may, of course, want to increase base-pairing stability to the point where duplexes of any sequence are formed with the stability of those between all-G/C sequences. While in medicinal chemistry, tighter binding is almost universally hailed as an improvement, the same is not necessarily the case for probing specific sequences in genomic DNA on microarrays. If one was to increase the affinity such that even short stretches of nucleotides suffice to form stable duplexes close to the boiling point of an aqueous buffer, false positives would again be difficult to suppress, as these short sequences are not sufficiently unique in a target genome to ensure the selectivity required for detecting typical genes, let alone genes coding for members of families of homologous proteins. Since it takes approximately 16 nucleotides in length to be statistically unique in the human genome, hybridization probes shorter than those employed here cannot be expected to be suitable for genome-wide analyses.

Oligonucleotide probes are used for binding target regions against a genomic sequence background in biomolecular applications ranging from those frequently discussed for microarrays, such as gene expression profiling, SNP detection, DNA copy number determination, alternative splicing analysis, and epigenomics to those involving duplex formation in solution, such as antisense, antigene, chimeraplasty, and RNA interference. Isostable DNA may prove beneficial for several of these applications, as it may reduce the need to optimize binding properties each time a new sequence is being targeted. But, additional experiments are needed to confirm the validity of this approach.

The current results provide a concept for undertaking such experiments, as they predict that a combination of (i) additional ligands interrogating the target strand, (ii) a stiffening of the duplex, and (iii) retention of the negatively charged DNA backbone is beneficial for high fidelity detection of target strands via isostable duplexes. It is hoped that our concept can serve as a blueprint for future designs and offers a framework for theoretical predictions.

Conclusions

In conclusion, the current results show that it is possible to adjust duplex stabilities for oligodeoxynucleotides to and beyond the same melting point with decorated nucleic acids, even for the extreme case of all-A/T and all-G/C sequences. This was demonstrated in solution and on microarrays of low and high spot density. In our approach, only one of the two strand is being modified, so that unmodified target strands may be detected. Isostable DNA duplexes allow for the use of universally stringent conditions that should lead to higher fidelity in the sequence-specific detection of diverse target strands under multiplexing conditions. Predictable hybridization equilibria should allow for in silico optimization of hybridization conditions, further reducing the need for conventional, low-fidelity experiments.

Experimental Section

General. Unless noted otherwise, chemicals were purchased from Acros (Geel, Belgium), Aldrich/Fluka/Sigma (Deisenhofen, Germany), or Merck (Darmstadt, Germany). Reagents for amide coupling, including *O*-benzotriazol-1-yl-*N*,*N*,*N*′,*N*′-tetramethyluronium hexafluorophosphate (HBTU) and 1-hydroxybenzotriazole (HOBT) as well as Boc-Lys-(TFA)-OH, were from Advanced ChemTech (Louisville, KY) and were used without purification. The 2-cyanoethyl-*N*,*N*-diisopropylchlorophosphoramidite for phosphitylations was obtained from TRC (North York, Canada). Underivatized long-chain alkylamine controlled pore glass (LCAA cpg) with a loading capacity of 78 μmol/g was from Controlled Pore Glass, Inc. (Lincoln Park, NJ). Anhydrous solvents were ordered and stored over molecular sieves and used without further purification. Standard phosphoramidites (dA^{Bz}, dC^{Bz}, T, dG^{dmf}), the phosphoramidites of locked nucleic acid monomers and the chemicals for DNA synthesis, including dicyanoimidazole (DCI) activator, were from Proligo (Hamburg, Germany), except for dG^{dmf}-loaded controlled pore glass (cpg), which was from ABI (Warrington, U.K.). Further, the phosphoramidites of *N*-4-ethyl-2′-deoxycytidine and 2′-deoxy-5′-dimethoxytrityl-5-iodouridine were obtained from ChemGenes (Wilmington, MA), whereas the phosphoramidite of Cy3 and 2′-deoxyinosine were from Glen Research (Sterling, VA). The 3′-*O*-yl-cyanoethyl-*N*,*N*-diisopropylphosphoramidite of 2′-(anthraquinone-*N*-methylcarboxamido)-2′-deoxy-5′-*O*-(4,4′-dimethoxytrityl)uridine (**8**) was synthesized as reported.[66] The synthesis of the phosphoramidites of trimethoxystilbene[61] and 3,6,9-trioxydecylamine[68] also followed known protocols. The LNA phosphoramidites, namely compound **10** and **11**, were obtained from Glen Research (Sterling, VA), and were used without modification. Their synthesis has been described in the literature.[46b] Aldehyde-coated glass slides were from Genetix Ltd. (New Milton, U.K.). Phosphate buffered saline solution (PBS, pH 7), 20-fold concentrated saline sodium citrate (SSC, pH 7.4), and 2-(*N*-morpholino)-ethanesulfonic acid buffer (MES, pH 6.3) were prepared using standard protocols.[88]

The unmodified oligonucleotides **compGC 27**, **27a**, **27b**, **27c**, **27d**, **27e**, **27f**, **27g**, **27h**, and **27i** and the Cy3-labeled oligonucleotide **compGCCy 28** were purchased from Operon Biotechnologies GmbH (Cologne, Germany) or VBC-Genomics (Vienna, Austria) in HPLC-purified form. The buildings blocks for the assembly of the DP-Lys-loaded cpg and the loaded support itself were generated following protocols published earlier.[67] Oligonucleotides were purified via reversed phase HPLC on Nucleosil columns (C4 or C18; both 250 mm $\times$ 4.6 mm by Macherey Nagel, Düren, Germany). Unless otherwise noted, this involved a gradient of CH_3CN (B) in 0.1 M triethylammonium acetate (pH 7.0) and detection at 260 nm. Yields of oligonucleotides are based on the integration of the HPLC trace of crude products. The integration was not corrected for the absorbance caused by the solvent front. Extinction coefficients for oligonucleotides were calculated through linear combination of the extinction coefficients of the nucleotides and are uncorrected for hyperchromicity effects. For modified oligonucleotides, the extinction coefficients were calculated as the sum of the extinction coefficient of the unmodified oligonucleotide and the extinction coefficient of the covalently linked chromophores. NMR spectra were acquired on a Bruker AC 250, AVANCE 400, or AVANCE 500 spectrometer. MALDI-TOF−MS spectra were acquired on a Bruker REFLEX IV spectrometer in negative, linear mode using the software XACQ 4.0.4 and XTof 5.1. The matrix was a mixture of 2,4,6-trihydroxyacetophenone (THAP, 0.2 M in ethanol) and diammonium citrate (0.1 M in water) (2:1, v/v). Calculated masses are average masses, and *m*/*z* found are those of the unresolved isotope envelopes of the pseudomolecular ions ($[M - H]^-$). DNA sequences are given 5′- to 3′-terminus.

1-*N*-(Propin-3-yl)-4-(pyren-1-yl)butyramide (4). To a stirred solution of 1-pyrene-4-butyric acid (**2**) (640 mg, 2.22 mmol) in DMF (5 mL) were added HOBt (408 mg, 2.66 mmol) and EDC (467 μL, 413 mg, 2.66 mmol). After 10 min at room temperature, propargylamine (171 μL, 147 mg, 2.66 mmol) was added slowly. The mixture was

(88) Sambrook, J.; Fritsch, E. F.; Maniatis, T. *Molecular cloning—a Laboratory Manual*, 2nd ed.; Cold Spring Harbor Laboratory: Cold Spring Harbor, New York, 1989.

stirred for 16 h, taken up in CH_2Cl_2 (70 mL), and washed thrice each with aqueous HCl (1 M, 70 mL), aqueous NaOH (1 M, 70 mL), and brine (70 mL). The organic layer was dried over Na_2SO_4 and evaporated in vacuo. Recrystallization from EtOH gave the title compound as a yellow solid (548 mg, 1.9 mmol, 76%). $R_f = 0.8$, $CHCl_3$/MeOH 9:1. ^{1}H NMR (250 MHz; $CDCl_3$): δ (ppm) = 2.13 (m, 5H), 3.30 (t, J = 7.4 Hz, 2H), 3.96 (m, 2H), 5.52 (bs, 1H), 7.72−8.26 (m, 9H). ^{13}C NMR (100.6 MHz; $CDCl_3$): δ (ppm) = 27.20, 29.21, 32.65, 35.64, 71.63, 79.56, 123.37, 124.82, 124.97, 125.00, 125.12, 125.90, 126.77, 127.40, 127.47, 127.49, 128.81, 130.01, 130.92, 131.44, 135.69, 172.17. HR-FAB-MS (3-NBA) calcd for $C_{23}H_{19}NO$, 325.1467; found, 325.1469.

5′-*O*-(4,4′-Dimethoxytrityl)-5-(3-(4-(pyren-1-yl)butyramido)propin-1-yl)-2′-deoxyuridine (6). 5′-*O*-(4,4′-Dimethoxytrityl)-5-iodo-2′-deoxyuridine (312 mg, 0.48 mmol) was dissolved in DMF (2.5 mL). The solution was degassed in vacuo and the flask flushed with argon. Then, NEt_3 (321 μL, 231 mg, 2.29 mmol), compound **4** (465 mg, 1.43 mmol), tetrakis(triphenylphosphine)palladium (55 mg, 48 μmol), and copper iodide (20 mg, 0.10 mmol) were added. In each case, the mixture was stirred until a clear solution was obtained before the next compound was added. After 4 h at room temperature, the mixture was diluted with ethyl acetate (70 mL) and washed thrice with aqueous EDTA solution (5%, 70 mL) and brine (70 mL). The organic layer was dried over Na_2SO_4 and the solvent was removed in vacuo. The yellow residue was purified by column chromatography (silica, pretreated with eluant containing 0.5% NEt_3, CH_2Cl_2/MeOH 93:7, $R_f = 0.29$) to give the title compound as a slightly yellow solid (375 mg, 439 μmol, 92%). ^{1}H NMR (500 MHz; $CDCl_3$): δ (ppm) = 1.96 (t, J = 7.2 Hz, 2H), 2.05 − 2.13 (m, 2H), 2.19−2.56 (m, 1H), 2.41−2.48 (m, 1H), 2.70 (bs, 1H), 3.25 (dd, J = 10.8 Hz, J = 3.3 Hz, 1H), 3.28−3.32 (m, 2H), 3.39 (dd, J = 10.8 Hz, J = 2.7 Hz, 1H), 3.72 (s, 6H), 3.85−3.99 (m, 2H), 4.03−4.07 (m, 1H), 4.43−4.48 (m, 1H), 5.35−5.40 (m, 1H), 6.28 (t, J = 6.3 Hz, 1H), 6.76−6.81 (m, 4H), 7.16−7.20 (m, 1H), 7.22−7.27 (m, 6H), 7.33−7.37 (m, 2H), 7.82 (d, J = 7.9 Hz, 1H), 7.95−8.01 (m, 3H), 8.06−8.10 (m, 2H), 8.12−8.18 (m, 3H), 8.26 (d, J = 9.1 Hz, 1H), 9.11 (bs, 1H). ^{13}C NMR (100.6 MHz; $CDCl_3$): δ (ppm) = 27.06, 29.94, 32.67, 35.37, 41.57, 55.27, 63.43, 72.15, 74.12, 85.74, 86.64, 87.06, 89.55, 99.56, 113.36, 123.38, 124.78, 124.90, 124.93, 125.04, 125.84, 126.70, 127.00, 127.32, 127.38, 127.46, 127.84, 128.07, 128.75, 129.90, 129.97, 130.87, 131.37, 135.33, 135.49, 135.83, 142.98, 144.51, 149.09, 158.58, 158.61, 161.73, 172.04. HR-FAB-MS (3-NBA) calcd for $C_{53}H_{47}N_3O_8$, 853.3363; found, 853.3365.

5′-*O*-(4,4′-Dimethoxytrityl)-5-(3-[4-(pyren-1-yl)butyramido]propin-1-yl)-2′-deoxyuridin-3′-*O*-yl-cyanoethyl-*N*,*N*-diisopropylphosphoramidite (1). Compound **6** (150 mg, 0.175 mmol) was dried for 16 h at 0.1 Torr, suspended in CH_3CN (900 μL), and treated with DIEA (92 μL, 68 mg, 0.526 mmol). To the stirred suspension, 2-cyanoethyl-*N*,*N*-diisopropylchlorophosphoramidite (51 μL, 54 mg, 0.228 mmol) was added. After 15 min at room temperature, a clear, slightly yellow solution formed, which was diluted with CH_2Cl_2 (30 mL) and washed twice with saturated aqueous $NaHCO_3$ (30 mL) and brine (30 mL), respectively. The organic layer was dried over Na_2SO_4 and concentrated to a volume of approximately 0.5 mL. The solution was added dropwise to cyclohexane (20 mL), leading to an off-white precipitate. After centrifugation, the supernatant was aspired, and the solid was purified by column chromatography (silica, pretreated with eluant containing 0.5% NEt_3, elution with acetone/cyclohexane 1:1, $R_f = 0.25$) to give **1** as a slightly yellow solid (175.6 mg, 0.166 mmol, 95%). ^{31}P NMR (202 MHz; $CDCl_3$): δ (ppm) = 149.3, 149.7. MALDI-TOF MS (THAP, linear positive mode) 1050.6.

Automated DNA Chain Assembly. The assembly of the unmodified portion of oligodeoxynucleotide was performed on 1 μmol scale, following the protocol recommended by the manufacturer of the synthesizer (8909 Expedite synthesizer, Perseptive Biosystems, system software 2.01), using a polypropylene reaction chamber for DNA synthesis (Prime Synthesis, Aston, PA). Phosphoramidites of modified residues were coupled with elongated coupling times of 3−9 min, where the latter value was employed for LNA phosphoramidites, as recommended by the suppliers.

Manual Chain Extension (General Protocol A). The solid support (cpg) and the phosphoramidite (20−30 equiv) were dried at 0.1 Torr in a polypropylene vessel. A solution of 1-*H*-tetrazole (0.45 M in CH_3CN, 50−200 μL, depending on the scale) was added, and the reaction mixture was shaken on a vortexer at low speed for 1 h at room temperature. After washing with CH_3CN and CH_2Cl_2, oxidizer solution for DNA synthesis (0.5 mL) was added, followed by shaking for 15 min at room temperature. The cpg was washed with CH_3CN, DMF, MeOH, and CH_2Cl_2, and was dried at 0.1 Torr, followed by continuation of the DNA synthesis or deprotection.

Deprotection and Cleavage of Oligonucleotides from cpg (General Protocol B). At the end of DNA syntheses, the cpg was briefly dried (0.1 Torr) and treated with saturated aqueous NH_3 (1 mL) for 16 h at room temperature or 3 h at 55 °C. The supernatant was transferred to a new vessel, and the solid support was washed with water (2 × 0.3 mL). Excess ammonia in the combined aqueous solution was removed with a gentle stream of compressed air. The solution was filtered and then used directly for HPLC purification.

Detritylation of Oligonucleotides During Purification (General Protocol C). The removal of DMT or MMT groups on the 5′-terminal nucleotide was achieved on a C-18 cartridge (Sep-Pak Vac 3 cm^3, 500 mg, Milford, MA). The cartridge was first washed with CH_3CN (4 mL) and TEAA buffer (triethylammonium acetate, 0.1 M, pH 7, 6 mL). The cartridge was loaded with the oligonucleotide dissolved in water or TEAA buffer. Then, TEAA buffer (2 mL), trifluoroacetic acid solution (0.2% in H_2O, 4 mL), and TEAA buffer (4 mL) were passed through the cartridge. The oligonucleotide was eluted with CH_3CN/TEAA (3:2, v/v, 4 mL) and CH_3CN/TEAA (9:1, v/v, 4 mL). Fractions were analyzed by MALDI-TOF−MS, and those containing pure product were combined and repeatedly lyophilized from water to remove the buffer.

AT2CapPyLNA, 5′-TMS-TAAU^{Py}T^{L}T^{L}U^{Py}T^{L}A^{L}A^{L}U^{Py}AAU$_{AQ}$-DP-Lys-3′ (12). Starting from solid support **9**, a manual coupling cycle with **8** according to general protocol A was performed, followed by automated DNA synthesis with standard phosphoramidites and **1**, **10**, and **11**. Next, phosphoramidite **7** was coupled manually according to general protocol A, followed by cleavage of the oligonucleotide from solid support according to general protocol B. Crude **12** was dissolved in 0.1 M LiOH with 20% CH_3CN and HPLC purified on a C-18 column with a gradient of CH_3CN (20−70% in 40 min; R_t = 23 min), yield of 40%. MALDI-TOF MS m/z $[M - H]^-$ calcd for $C_{258}H_{273}N_{53}O_{108}P_{15}$, 6308.5; found, 6307.5.

AT, 5′-TAATTTTTAATAAT-DP-Lys-3′ (13). Prepared on solid support **9** by standard DNA synthesis, deprotection (general protocol B), and HPLC purification (C-18 column) with a gradient of 0% CH_3CN for 5 min, to 20% in 55 min; R_t = 49 min, yield of 35%. MALDI-TOF MS m/z $[M - H]^-$ calcd for $C_{151}H_{197}N_{48}O_{90}P_{14}$, 4558.1; found, 4559.1.

ATCap, 5′-TMS-TAATTTTTAATAAT-DP-Lys-3′ (14). Synthesized on support **9** with phosphoramidite **7** (general protocol A), followed by cleavage (general protocol B) and HPLC purification (C-18 column) with a gradient of 0% CH_3CN for 5 min, to 25% in 30 min; R_t = 31 min, yield of 66%. MALDI-TOF MS m/z $[M - H]^-$ calcd for $C_{172}H_{221}N_{49}O_{97}P_{15}$, 4991.5; found, 4989.2.

AT2Cap, 5′-TMS-TAATTTTTAATAAU$_{AQ}$-DP-Lys-3′ (15). Starting from solid support **9** phosphoramidite **8** was coupled (general protocol A), followed by standard DNA synthesis, coupling of phosphoramidite **7** (general protocol A), and cleavage (general protocol B). HPLC purification (C-18 column) with a gradient of 0% B for 5 min, to 35% in 40 min; R_t = 32 min, yield of 45%. MALDI-TOF MS m/z $[M - H]^-$ calcd for $C_{187}H_{228}N_{50}O_{100}P_{15}$, 5240.7; found, 5240.1.

AT2CapPy, 5′-TMS-TAATTTU^{Py}TAAU^{Py}AAU$_{AQ}$-DP-Lys-3′ (16). Synthesized identically to **15**, except that phosphoramidite **1** was also used in manual coupling steps (general protocol A). HPLC (C-18 column) with a gradient of 0% B for 5 min, to 35% in 40 min; R_t =

40 min, yield of 24%. MALDI-TOF MS *m/z* [M − H]$^-$ calcd for $C_{231}H_{258}N_{52}O_{102}P_{15}$, 5859.2; found, 5857.0.

compAT, 5′-ATTATTAAAAATTA-3′ (17). Assembled via standard DNA synthesis, cleaved from solid support according to the general protocol B, and HPLC purified (C-18 column) with a gradient of 0% B for 5 min, to 18% in 35 min; R_t = 38 min, yield of 66%. MALDI-TOF MS *m/z* [M − H]$^-$ calcd for $C_{140}H_{175}N_{52}O_{80}P_{13}$, 4268.9; found, 4268.4.

compATCy, 5′-Cy3-ATTATTAAAAATTA-3′ (18). Synthesized via standard DNA synthesis followed by manual coupling of the Cy3-phosphoramidite (general protocol A) and removal of the MMT group (general protocol C). After cleavage from solid support (general protocol B), HPLC purification (C-4 column) with a gradient of 0% B for 5 min, to 30% in 25 min; R_t = 29 min, yield of 46%. MALDI-TOF MS *m/z* [M − H]$^-$ calcd for $C_{169}H_{211}N_{54}O_{84}P_{14}$, 4776.5; found, 4773.6.

LNACap, 5′-A^{L}GGTTGAC-3′ (19). Chain assembly by standard DNA synthesis, followed by manual coupling of phosphoramidite **10** (general protocol A), deprotection (general protocol B), and HPLC purification (C-18 column) with a gradient of 0% B for 5 min, to 18% in 25 min; R_t = 30 min, yield of 82%. MALDI-TOF MS *m/z* [M − H]$^-$ calcd for $C_{80}H_{99}N_{32}O_{47}P_7$, 2477.6; found, 2472.8.

LNACapcon, 5′-AGGTTGAC-3′ (20). Synthesized via standard DNA synthesis, cleavage (general protocol B), and HPLC purification (C-18 column) with a gradient of 0% B for 5 min, to 18% in 25 min; R_t = 29 min, yield of 72%. MALDI-TOF MS *m/z* [M − H]$^-$ calcd for $C_{79}H_{99}N_{32}O_{46}P_7$, 2449.7; found, 2449.3.

compLNACap_A, 5′-GTCAACCA-3′ (21a). Synthesized analogously to **20**, HPLC purification (C-18 column) with a gradient of 0% B for 5 min, to 18% in 30 min; R_t = 30 min, yield of 75%. MALDI-TOF MS *m/z* [M − H]$^-$ calcd for $C_{77}H_{98}N_{31}O_{44}P_7$, 2378.6; found, 2378.1.

compLNACap_C, 5′-GTCAACCC-3′ (21c). Synthesized analogously to **20**, HPLC purification (C-18 column) with a gradient of 0% B for 5 min, to 18% in 30 min; R_t = 29 min, yield of 81%. MALDI-TOF MS *m/z* [M − H]$^-$ calcd for $C_{76}H_{98}N_{29}O_{45}P_7$, 2354.6; found, 2354.4.

compLNACap_G, 5′-GTCAACCG-3′ (21g). Synthesized analogously to **20**, HPLC purification (C-18 column) with a gradient of 0% B for 5 min, to 18% in 30 min; R_t = 30 min, yield of 74%. MALDI-TOF MS *m/z* [M − H]$^-$ calcd for $C_{77}H_{98}N_{31}O_{45}P_7$, 2394.6; found, 2394.2.

compLNACap, 5′-GTCAACCT-3′ (21t). Synthesized analogously to **20**, HPLC purification (C-18 column) with a gradient of 0% B for 5 min, to 18% in 30 min; R_t = 30 min, yield of 89%. MALDI-TOF MS *m/z* [M − H]$^-$ calcd for $C_{77}H_{99}N_{28}O_{46}P_7$, 2369.6; found, 2368.9.

GC, 5′-CGGCCCCCGGCGGC-DP-Lys-3′ (22). Assembled on support **9** via standard DNA synthesis, followed by cleavage (general protocol B) and HPLC purification (C-18 column) with a gradient of 0% B for 5 min, to 20% in 40 min; R_t = 38 min, yield of 20%. MALDI-TOF MS *m/z* [M − H]$^-$ calcd for $C_{143}H_{189}N_{56}O_{88}P_{14}$, 4534.0; found, 4527.3.

GC3Et, 5′-CGGC^{Et}CCC^{Et}CGGC^{Et}GGC-DP-Lys-3′ (23). Prepared on support **9** via a standard DNA synthesis, including the 3′-phosphoramidite of 2′-deoxy-*N*-4-ethylcytidine, followed by cleavage (general protocol B) and HPLC purification (C-18 column) with a gradient of 0% B for 5 min, to 30% in 35 min; R_t = 25 min, yield of 38%. MALDI-TOF MS *m/z* [M − H]$^-$ calcd for $C_{149}H_{201}N_{56}O_{88}P_{14}$, 4618.2; found, 4617.5.

GC3I, 5′-CIGCCCCCIGCGIC-DP-Lys-3′ (24). Synthesized on support **9** via automated synthesis involving the 3′-phosphoramidite of 2′-deoxyinosine, followed by cleavage (general protocol B) and HPLC purification (C-18 column) with a gradient of 0% B for 5 min, to 19% in 35 min; R_t = 32 min, yield of 64%. MALDI-TOF MS *m/z* [M − H]$^-$ calcd for $C_{143}H_{186}N_{53}O_{88}P_{14}$, 4489.0; found, 4487.9.

GC3EtCI, 5′-CIGC^{Et}CCC^{Et}CIGC^{Et}GIC-DP-Lys-3′ (25). Starting from **9**, **25** was synthesized via standard DNA synthesis involving the phosphoramidite building blocks of 2′-deoxyinosine and 2′-deoxy-*N*-4-ethylcytidine followed by cleavage (general protocol B) and HPLC purification (C-18 column) with a gradient of 0% B for 5 min, to 21% in 35 min; R_t = 31 min, yield of 41%. MALDI-TOF MS *m/z* [M − H]$^-$ calcd for $C_{149}H_{198}N_{53}O_{88}P_{14}$, 4573.7; found, 4571.2.

GC8CEt, 5′-C^{Et}GGC^{Et}C^{Et}C^{Et}C^{Et}C^{Et}GGC^{Et}GGC^{Et}-DP-Lys-3′ (26). The synthesis was analogous to that of **23**, except that the 5′-terminal DMT group was removed on-cartridge according to general protocol C subsequent to HPLC purification. HPLC (DMT-on, C-18 column), gradient of 0% B for 5 min, to 35% in 45 min; R_t = 43 min, yield of 70%. MALDI-TOF MS *m/z* [M − H]$^-$ calcd for $C_{159}H_{221}N_{56}O_{88}P_{14}$, 4758.4; found, 4756.0.

UV-Melting Curves. UV-melting curves were measured on a Perkin-Elmer Lambda 10 spectrophotometer with detection at 260 nm and gradients of 1 °C/min. Melting temperatures were determined with UV Winlab 2.0 (Perkin-Elmer), based on the extrema of the first derivative of the 91-point smoothed curves, and are averages of four measurements. Hyperchromicities were determined by calculating the difference in absorption between high- and low-temperature baseline and dividing by the low-temperature absorption. Thermodynamics of duplex formation were calculated by fitting with Meltwin.[75]

DNA Microarrays.

Slides. The slides were cleaned from dust in a stream of argon, washed with CH_2Cl_2 (50 mL, 10 min), ethanol (50 mL, 10 min), and distilled water (50 mL, 10 s), and dried in a stream of argon.

Manual Spotting. For immobilization, a solution of lysine-terminated oligonucleotides (1 μL, 10 μM DNA in 0.1 M MES buffer, 0.1 M glycerol) was applied to the slide surface without touching the surface. After 2 h at room temperature in a humid chamber, a solution of $NaBH_3CN$ (0.35 μL, 50 mM in PBS buffer) was added to the drops. After 1 h at room temperature, the droplets were removed by rinsing with buffer (10 mL, 1 × SSC/0.2% SDS) followed by washing by immersion into buffer (50 mL, 1 × SSC/0.2% SDS, 1 min and 50 mL, PBS, 1 min). The slide was used directly for passivation, without drying.

Automated Spotting. Solutions of the lysine-terminated oligonucleotides (1 μL, 10 μM DNA in 0.1 M MES buffer, 1 M glycerol) were applied to the slide surface using a genemachine Omnigrid 100 with SMP 3 pins (Genemachines/Genomic Solutions, Ann Arbor, MI). Approximately 0.25 nL was applied per spot. After incubation for 16 h at room temperature in a humid chamber, the droplets were removed by rinsing with buffer (10 mL, 1 × SSC/0.2% SDS) followed by washing with buffer (50 mL, 1 × SSC/0.2% SDS, 1 min and 50 mL, PBS, 1 min). The slides were then used directly for passivation without drying.

Background Passivation. Remaining aldehyde groups on the surface were reacted with 3,6,9-trioxydecylamine[68] (10 mM solution in PBS buffer), and the resulting imino linkages reduced with $NaBH_3CN$ (50 mM in the solution applied). After incubation for 3 h at room temperature, the slide was washed with buffer (50 mL, 1 × SSC/0.2% SDS, 1 min), twice with water (50 mL each, 10 s), and dried in a stream of argon.

Hybridization. For hybridization, a solution containing the Cy3-labeled target strands (30 μL, 10 μM DNA, 2 × SSC buffer, 0.2% SDS) was applied to the slide surface under a cover slip. The slide was stored in an incubation chamber (Peqlab-Biotechnologie, Erlangen, Germany) at the desired temperature with sufficient humidity to avoid drying. The slide was washed by immersion into buffer (50 mL, 1 × SSC/0.2% SDS) at the same temperature as that used for hybridization. A second washing step involved buffer (50 mL, 1 × SSC) at room temperature. The slide was then immediately dried in a stream of argon.

Fluorescence Scans and Data Analysis. The read-out of the fluorescence signals from the spots of the slides was performed with

an ArrayWoR$_x^e$ Biochip Reader (GeneScan, Freiburg, Germany). The exposure time was set to 0.10 s. Fluorescence of Cy3 was detected by using the following filters: 546 ± 5 nm (excitation); 575 ± 30 nm (emission). The fluorescence reading for Cy5-labeled oligonucleotides performed during control studies involved the following settings: excitation at 640/20 nm and detection at 680/30 nm. The analysis of images was performed using the ArrayWoR$_x^e$ analysis software. The diameter of the area analyzed for each spot was set to a value slightly below the real diameter (e.g., 0.9 mm diameter for manually spotted arrays) to avoid integration of background signal. Unless noted otherwise, the signal of the background was subtracted from the signals for individual spots.

Acknowledgment. The authors are grateful to M. Bauer for spotting high-density microarrays, to S. Al-Rawi for providing synthetic intermediates, to A. Patra for mass spectrometric data, to J. Rojas Stütz, U. Plutowski, P. Baumhof, and K. Giessler for helpful discussions, to S. Lumpp and A. Hochgesand for expert technical assistance, and to P. Grünefeld, K. Imhof, E. Kervio, and M. Röthlingshöfer for a review of the manuscript. This study was supported by DFG (FOR 434 and RI 1063/4-4).

Supporting Information Available: Complete refs 19, 20, and 28; reaction scheme for immobilization of probe strands on slides; thermodynamics of duplex formation; data on saturation for microarrays; calculated binding curves and experimental data for high-density microarray; NMR spectra; and MALDI-TOF mass spectra. This material is available free of charge via the Internet at http://pubs.acs.org.

JA074209P